THE JOURNAL OF COMPARATIVE NEUROLOGY 374:204–222 (1996)

GABAergic Inputs to the Nucleus Rotundus (Pulvinar Inferior) of the Pigeon (*Columba livia*)

JORGE MPODOZIS, KEVIN COX, TORU SHIMIZU, HANS-JOACHIM BISCHOF, WALTER WOODSON, AND HARVEY J. KARTEN

Facultad de Ciencias, Universidad de Chile, Casilla 653 Santiago, Chile (J.M.); Department of Neurosciences, University of California, San Diego, La Jolla, California 92093-0608 (K.C., H.J.K.); Department of Psychology, University of South Florida, Tampa, Florida 337620-8200 (T.S.); Fakultat Biologie, Universitat Bielefeld, Postfach 100131 Bielefeld, Germany (H.-J.B.); and Center for Neural Sciences, New York University, New York, New York 10003 (W.W.)

ABSTRACT

The avian nucleus rotundus, a nucleus that appears to be homologous to the inferior/caudal pulvinar of mammals, is the major target of an ascending retino-tecto-thalamic pathway. Further clarification of the inputs to the rotundus and their functional properties will contribute to our understanding of the fundamental role of the ascending tectal inputs to the telencephalon in all vertebrates, including mammals.

We found that the rotundus contains a massive plexus of glutamic acid decarboxylase (GAD)-immunoreactive axons using antibodies against GAD. The cells within the rotundus, however, were not immunoreactive for GAD. The retrograde tracer cholera toxin B fragment was injected into the rotundus to establish the location of the afferent neurons and determine the source of the gamma-aminobutyric acid (GABA) inputs into the rotundus. In addition to the recognized bilateral inputs from layer 13 of the tectum, we found intense retrograde labeling of neurons within the ipsilateral nuclei subpretectalis (SP), subpretectalis-caudalis (SPcd), interstitio-pretecto-subpretectalis (IPS), posteroventralis thalami (PV), and reticularis superior thalami (RS). All the neurons of the SP, SPcd, IPS, and PV were intensely GAD-immunoreactive. The neurons of layer 13 of the tectum were not immunoreactive for GAD.

Following the destruction of the ipsilateral SP/IPS complex, we found a major reduction in the intensity of the GAD axonal immunoreactivity within the ipsilateral rotundus, but this destruction did not diminish the intensity of the GAD-immunoreactivity within the contralateral rotundus.

Our studies indicated that the source of the massive GAD-immunoreactive plexus within the rotundus was from the ipsilateral SP, SPcd, IPS, and PV nuclei. These nuclei, in turn, received ipsilateral tectal input via collaterals of the neurons of layer 13 in the course of their projections upon the rotundus.

We suggest that the direct bilateral tecto-rotundal projections are excitatory, whereas the indirect ipsilateral projections from the SP/IPS and PV are mainly inhibitory, possibly acting via a GABA-A receptor.

Indexing terms: tectofugal system, pretectum, visual system, evolution, birds

Many of the visual discrimination and recognition functions attributed to the retino-geniculo-striate cortex system in mammals are also performed by birds and other vertebrates. There are, however, major differences between the systems used by mammalian and nonmammalian vertebrates to perform these functions. One of the most striking differences is related to the relative size of the different retinal projections. In most mammals, the retino-geniculo-striate cortex receives the major proportion of the retinal inputs. By comparison, the homologous retino-opticus principalis thalami (OPT)-wulst system found in most birds receives only a small proportion of the retinal input. In birds and other nonmammalian vertebrates, it is the optic

Accepted May 16, 1996.

Address reprint requests to Dr. Harvey J. Karten, Department of Neurosciences-0608, University of California, San Diego, La Jolla, CA 92093-0608. E-mail: kartenh@sdsc.edu

tectum that is the main recipient of the retinal inputs and is the central origin of a massive ascending polysynaptic pathway upon the telencephalon. This sequence of connections is referred to by Karten and Hodos (1970) as the "tectofugal pathway." The prominent tectofugal pathway in pigeons provides a useful model for understanding the original role of ascending tectal projections to the telencephalon in all vertebrates, including mammals.

The target of the ascending tectal projections from the optic tectum in birds and reptiles is the nucleus rotundus, the largest single nucleus in the thalamus of most birds and reptiles.

The rotundus of pigeons receives a major bilateral projection from the stratum griseum centrale (SGC), also designated as layer 13, of the optic tectum (Karten and Revzin, 1966; Benowitz and Karten, 1976; Hunt and Künzle, 1976; Engelage and Bischof, 1993). Efferent projections from the rotundus project exclusively upon the ipsilateral telencephalon, terminating within a relatively homogeneous field of neurons designated as the ectostriatal core (Karten and Hodos, 1970). The ectostriatal core projects upon a sequential array of cell groups, with the eventual descending projections from the archistriatum intermedium, pars ventrolateralis (Aivl) upon the optic tectum, terminating within layers 11-13 of the tectum (Karten et al., 1993).

Anatomical and behavioral studies have revealed that the rotundal projection upon the telencephalon is the major system mediating visual discrimination in most birds and reptiles (Hodos and Karten, 1966, 1970; Reiner and Powers, 1980; Shimizu and Karten, 1991). Similar studies of visual pathways in many mammals, including the tree shrew, squirrel, and primates, indicate that the tecto-rotundal pathway is also a major component of the ascending visual pathways to the temporal cortex and is vital in the performance of visual discrimination (Raczkowski and Diamond, 1978, 1981). The avian nucleus rotundus appears to be homologous to the inferior/caudal pulvinar of many mammals based on a number of corresponding features (Diamond, 1973; Shimizu and Karten, 1991).

Physiologic studies of the rotundus have yielded a series of confounding observations. Foremost among them has been the apparent absence of retinotopic organization within the rotundus. This has been all the more puzzling in light of the precise retinotopy characteristic of the optic tectum. Rotundal neurons have large receptive fields (often greater than 100 degrees) and are exquisitely sensitive to motion in the X, Y, and Z planes to displacements of 15 minutes of arc or less (Lettvin, personal communication; Revzin, 1979; Wang et al., 1993). Various subdivisions of the rotundus in birds show selective responses to luminance, color, and direction of motion (Granda and Yazulla, 1971; Revzin, 1979; Wang et al., 1993).

To identify the functional properties of the inputs to the rotundus, we surveyed the nucleus rotundus for the presence of various neuroactive substances. The present report outlines our findings regarding the presence of large quantities of glutamic acid decarboxylase (GAD) within the rotundus and the source of such inputs. In the course of these studies, we also began a re-evaluation of the inputs to the rotundus from the optic tectum using retrograde and anterograde tracers of greater sensitivity than available at the time of our earlier studies of this system. These more sensitive tracers indicated that the rotundus may receive a bisynaptic input from the retina, a much more direct and tightly linked input than previously appreciated that will be described in a separate report. A preliminary description of these results was previously reported in abstract form (Shimizu et al., 1988; Karten et al., 1993).

MATERIALS AND METHODS

This study used white Carneaux pigeons of either sex obtained from either Palmetto Pigeon Plant (Sumter, SC) or Bowman Gray School of Medicine (Winston-Salem, NC). All procedures used were approved by the Animal Care Committee of the University of California, San Diego, and conform to the guidelines of the National Institutes of Health on Use of Experimental Animals in Research.

In addition to the experimental group of animals specifically used in these studies, we also reviewed our collection of slides of previous experimental studies of pigeons with injections of various tracers, including horseradish peroxidase, cholera toxin B unit, *Phaseolus vulgaris* leucoagglutinin, and tritiated amino acids, located within the optic tectum, the ventral nucleus of the lateral geniculate, and various regions of the telencephalon.

Pigeons were anesthetized with a combination of ketamine (40 mg/kg) and xylazine (12 mg/kg) injected intra-

Abbreviations

Aivl	archistriatum intermedium, pars ventrolateralis
AL	ansa lenticularis
CO	chiasma opticum
CT	commissura tectalis
DLL	nucleus dorsolateralis anterior thalami, pars lateralis
FPL	fasciculus prosencephali lateralis
GAD-IR	glutamic acid decarboxylase-immunoreative
GCt	substantia grisea centrale
GLv	nucleus geniculatus lateralis, pars ventralis
IPS	nucleus interstitio-pretecto-subpretectalis
nBOR	nucleus of the basal optic root
OPT	nucleus opticus principalis thalami
Ov	nucleus ovoidalis
PST	tractus pretecto-subpretectalis
PT	nucleus pretectalis
PV	nucleus posteroventralis thalami
QF	tractus quintofrontalis
RSd	nucleus reticularis superior, pars dorsalis
RSv	nucleus reticularis superior, pars ventralis
Rt	fasciculus prosencephali lateralis
Rt/PI	nucleus rotundus/pulvinar inferior
RtCe	nucleus rotundus/pulvinar inferior, pars centralis
RtDa	nucleus rotundus/pulvinar inferior, pars dorsalis anterior
RtPost	nucleus rotundus/pulvinar inferior, pars posterior
RtTr	nucleus rotundus/pulvinar inferior, pars triangularis
Ru	nucleus ruber
SGC	tectum opticum, stratum griseum centrale
SGP	substantia grisea et fibrosa periventricularis
SP	nucleus subpretectalis
SPC	nucleus superficialis parvocellularis
SPcd	nucleus subpretectalis, pars caudalis
SP/IPS	ipsilateral nuclei subpretectalis/interstitio-pretecto-subpretectalis
SpL	nucleus spiriformis lateralis
SpM	nucleus spiriformis medialis
TeO	tectum opticum
TIO	isthmo-opticus tractus
TrO	tractus opticus
VSOD	decussatio supraoptica ventrale

muscularly. Effective anesthesia was usually achieved within 15 minutes. A single dose usually proved satisfactory for the duration of the surgical procedure. If necessary, a supplementary injection of ketamine and xylazine was administered.

Once the animal was anesthetized, the feathers over the skull were removed and the scalp washed with an antiseptic solution. Animals were placed in a stereotaxic head-holder with the skull exposed, and a hole was made through the skull above the approximate location of the injection.

Injections into the rotundus were achieved using stereotaxic coordinates (Karten and Hodos, 1967). To enhance the accuracy of placements of tracers within the rotundus, electrophysiologic responses were monitored. An insulated tungsten wire electrode was placed stereotaxically into the rotundus, and the coordinates were verified by the characteristic responses of rotundal cells (brisk movement sensitive, extremely wide receptive fields, minimal ON/OFF responses, minimal response to stationary stimuli) to various stimuli. Stimuli consisted of light from a small flashlight as well as hands and faces in various degrees of distortion attached to enthusiastic students and coauthors. The tungsten electrode was then withdrawn, and a glass micropipette filled with tracer was substituted and lowered to the same coordinates. In the course of these studies, we found that the use of pipettes with tip diameters of 10 to 20 mm, filled with a 1% (by weight) solution of cholera toxin B subunit (List Labs, Campbell, CA) made in phosphate-buffered saline (PBS), provided satisfactory recording electrodes, and the use of tungsten electrode was discontinued. The impedance of these cholera toxin B-filled pipettes was approximately 10 MΩ. These pipettes provided reasonable multi-unit recordings while still permitting large enough tip diameters to ensure release of tracers under moderate levels of pressure.

The pipettes were mounted in a dual-purpose holder that allowed both recording through the pipette and delivery of pulses of nitrogen gas under variable pressure using the PicoSpritzer II (General Valve, Fairfield, NJ). A silver/silver chloride wire was immersed in the cholera toxin B in the pipette and connected to a head stage of an AM preamplifier (AM Instruments, Everett, Washington). Signals were displayed on a Tektronix oscilloscope (Tektronix Inc., Beaverton, OR) and simultaneously monitored on an audio amplifier. The PicoSpritzer II was driven using a Grass stimulator (Grass Instruments, Quincy, MA) to deliver approximately 5 to 10 nl every 10 to 15 seconds, with a total duration sufficient to deposit approximately 50 to 250 nl of tracer.

In three additional animals, a phosphate buffered solution of 2.5% *Phaseolus vulgaris* leucoagglutinin (PHA-L) (Vector Labs, Burlingame, CA) was deposited at stereotaxically determined loci using iontophoresis, positive DC current, 4.5 mA for 30 to 40 minutes, with a constant current device (Midgard Electronics, Cambridge, MA; Gerfen and Sawchenko, 1983).

Following surgery and recovery from anesthesia, animals were maintained in the central animal resources facility and observed daily with attention to signs indicating infection. We found no evidence of infection at the operative sites. All animals were awake and alert within 30 to 60 minutes following completion of surgery and were able to feed and drink by the following morning.

Depending on the type of the tracer used, in 4 to 10 days the animals were anesthetized with an overdose of ketamine and xylazine and perfused via the aorta with 500 to 800 ml of 0.9% saline solution followed by 1000 ml of an ice cold solution of either 1% (for GAD immunohistochemistry) or 4% paraformaldehyde (for PHA-L and cholera toxin B immunohistochemistry) made in 0.1M phosphate buffer (PB, pH 7.2). A peristaltic perfusion pump was used to maintain constant perfusion pressure. Following the perfusion, the brains were removed and post-fixed for 6 to 14 hours in the paraformaldehyde solution and then transferred to a 30% sucrose solution made in PB for cryoprotection before cutting on a sliding microtome. The brains were cut into 30-μm thick sections in the horizontal, sagittal, or coronal plane.

The tissue was then washed in PBS for 30 minutes and then incubated in a primary solution consisting of PBS and 0.3% Triton X-100 and one of the following antibodies polyclonal rabbit GAD 1440 (1:2,000, provided by Dr. Wolfgang Oertel, Ludwig-Maximilians University, Munchen, Germany), monoclonal mouse GAD-2 (1:2,000, provided by Dr. David Gottlieb, Washington University School of Medicine, St. Louis, MO), rabbit anti-PHA-L (1:10,000, Vector Labs), or goat anti-cholera toxin B (1:15,000, List Labs), depending on the experiment. The tissue was incubated in the primary solution on a rotator, overnight at 4°C. Following a PBS wash, the tissue was incubated in a solution consisting of a biotinylated IgG antibody diluted 1:200 in PBS with 0.3% Triton X-100 (anti-sheep, GAD 1440; anti-mouse, GAD-2; anti-rabbit, PHA-L; or anti-goat, cholera toxin B) on a rotator for 1 hour at room temperature. Another PBS wash, and the tissue was incubated in the avidin-biotin-peroxidase complex (ABC Elite kit, Vector Labs), diluted 1:100 in PBS with an additional 2.9% sodium chloride added to reduce background and 0.3% Triton X-100 on a rotator for 1 hour at room temperature. After another wash in PBS, and the tissue was incubated in 0.25% 3-3' diaminobenzidine and 0.01% hydrogen peroxide in phosphate buffer until the appropriate signal to noise ratio was achieved. The tissue was then washed in PBS and mounted on gelatinized slides. On drying, the tissue was either stained with 0.04% osmium tetroxide for 10 to 20 seconds or counterstained with Giemsa stain (Iñiguez et al., 1985). The tissue was then dehydrated, cleared, and coverslipped with Permount.

Data analysis was performed by using a matched series of sections immunoreacted against cholera toxin B. One series was osmicated, and the other series counterstained with Giemsa. The two series were compared, and selected sections from each were drawn using a macroprojector. The distribution of axonal processes was frequently evaluated by using dark-field microscopy. Labeled neurons and axons were plotted on these drawings, and the resultant drawings were directly entered into a Mac IIfx data file by using an HP Desktop Scanner. The scanned drawing was traced by using Canvas 3.5 (Deneba Corp., Miami, FL). Additional sections were charted by using Neurolucida, a computer-controlled motorized stage and software system (MicroBrightfield Inc., Colchester, VT).

Photomicrographs, Figures 2, 7, 10, and 11, were taken by using a Nikon Microphot FX photomicroscope with Kodak TechPan 35 mm film and were printed by using standard darkroom methods. Photographs for Figures 4, 5, 6, 8, and 12 are digital images captured by using a Leaf Lumina scanning CCD camera (Leaf System Inc., Southborough, MA) mounted on a Nikon Microphot FX photomicroscope, and collected directly into Adobe Photoshop 3.0.1

(Adobe Systems Inc., Mountain View, CA) by using a Macintosh PowerPC 8100. Images were collected as RGB files, converted to grayscale images, and brightness and contrast adjusted to provide the resultant final printed images. No additional digital filtration or image modification was performed. Final prints were prepared by using a Kodak XLS 8600 PS printer.

RESULTS

Subdivisions within rotundus

Figure 1 is a series of drawings indicating the major subdivisions of the rotundus. These drawings are based on an examination of sections stained using cresyl violet, acetylcholinesterase, parvalbumin and calcium binding protein, the differential distribution of various transmitter related molecules, and the previously described differences in afferentation. For the purpose of the present study, our analysis concentrated on four main subdivisions: 1) pars dorsalis anterior, 2) pars centralis, 3) nucleus triangularis, and 4) pars posterior.

GAD Immunoreactivity within rotundus

Two different antibodies against GAD were used in this study: GAD 1440 (Oertel et al., 1981) and GAD-2 (Gottlieb et al., 1986), which recognize the isoforms 67 and 65 kDa, respectively. GAD 1440 produced moderately extensive staining of cell bodies, with variable staining of axons. GAD-2 provided excellent staining of processes, but only limited staining of cell bodies. The following description is a summary of our findings using both antibodies.

All subdivisions of the rotundus were intensely GAD-immunoreactive (IR) (Fig. 2). Staining was confined to axon-like processes. There was no indication of GAD-IR within any of the neurons within the rotundus. The axonal staining was generally organized in vertically oriented fascicles, entering from the base of the rotundus. The dorsal anterior subdivision of the rotundus appeared to be somewhat more intensely labeled than the other subdivisions.

Afferents to rotundus. To identify the sources of the GAD input to the rotundus, cholera toxin B was injected into various subdivisions of the rotundus, and the locus of the retrogradely labeled cell bodies was identified. Nuclei containing retrogradely cholera toxin B-labeled neurons were then compared with a library of brain sections immunoreacted for GAD.

Injections of cholera toxin B were restricted to the rotundus in ten animals. The following description will be limited to the six animals that had the most restricted injections within the rotundus. Injections sites were centered within the dorsal anterior (two cases), posterior (one case), centralis (dorsalis and ventralis) (two cases), and triangularis (one case) regions. An additional animal included in this description had an injection of cholera toxin B located within the ipsilateral ventral supraoptic decussation. The location of the injection sites for each of these regions is shown in Figure 3.

Following injections of tracer confined to the nucleus rotundus, retrogradely cholera toxin B labeled neurons were observed within three groups of neurons: 1) layer 13 of the ipsilateral and contralateral optic tectum; 2) the intrinsic cell groups lying within the ipsilateral tecto-thalamic tract including subpretectalis (SP), subpretectalis, pars caudale (SPcd), interstitio-pretecto-subpretectalis (IPS), and posteroventralis (PV); and 3) the ipsilateral nucleus reticularis superior diencephali, pars dorsalis and ventralis (RSd, RSv). There were no retrogradely cholera toxin B labeled neurons within the contralateral rotundus.

Optic tectum

Following injections restricted to the rotundus, the only population of neurons found to be retrogradely labeled with cholera toxin B within the optic tectum were the ipsilateral cells of layer 13/SGC (Fig. 4). A similar pattern of retrogradely labeled tectal neurons was observed in the contralateral optic tectum, although of lesser density. We found that layer 13 contained sublaminae, with differential projections upon individual subnuclei of the rotundus. Additional details regarding the cells and processes in layer 13 and the differential projections of both the ipsilateral and the contralateral tecti upon the rotundus are contained in a separate report.

Intrinsic Nuclei of the Tecto-Thalamic Tract. The SP, SPcd, IPS, and PV are distinct groups of intrinsic cells lying within the tecto-thalamic tract in the course of its trajectory from the tectum to the rotundus. They all receive tectal inputs and may properly be designated as intrinsic or "bed nuclei" of the tecto-thalamic tract. SP, SPcd, and IPS have also been grouped with the "pretectal" nuclear complex (Kuhlenbeck, 1939), although they neither receive retinal input nor do they project upon the optic tectum, but lie within the diencephalic-mesencephalic border designated as "pretectum."

Nucleus subpretectalis. Nucleus subpretectalis (SP) is a well-delineated cell group lying within the main bundle of axons of the tecto-rotundal tract. After injections of tracer into the dorsoanterior and central divisions of the rotundus, the neurons of the ipsilateral SP were intensely labeled with retrograde tracer. In addition, a dense plexus of axonal processes within SP was labeled bilaterally. There was no evident labeling of the ipsilateral or contralateral SP following injections of tracer into the pars triangularis or the pars posterior of the rotundus (Figs. 5 and 9).

Nucleus interstitio-pretecto-subpretectalis. Nucleus interstitio-pretecto-subpretectalis (IPS) forms a triangular cap on the dorsum of SP. The somata of IPS were intensely retrogradely cholera toxin B labeled on the ipsilateral side following tracer injections into the dorsoanterior and the central divisions of the rotundus (Figs. 5 and 9). As in SP, these injections resulted in bilateral axonal labeling within IPS. No other obvious topographic relationship was observed. IPS was not labeled ipsilaterally or contralaterally following cholera toxin B injections into pars triangularis or pars posterior of the rotundus.

Nucleus subpretectalis, pars caudale. Nucleus subpretectalis, pars caudale (SPcd) has not been previously described. SPcd lies interposed between the SP and the nucleus spiriformis lateralis (SpL) and extends along the caudomedial margin of SP proper. The cells of SPcd are approximately the same size as those of the SpL and may be erroneously considered a component of SpL, if the comparison were based only on relative cell size. SPcd may also be distinguished from the neurons of SpL, which are intensely immunoreactive for both leu-enkephalin (Reiner et al., 1982) and nicotinic acetylcholine receptor immunoreactivity (Swanson et al., 1983; Britto et al., 1992). Following unilateral injections of tracer confined to the pars triangula-

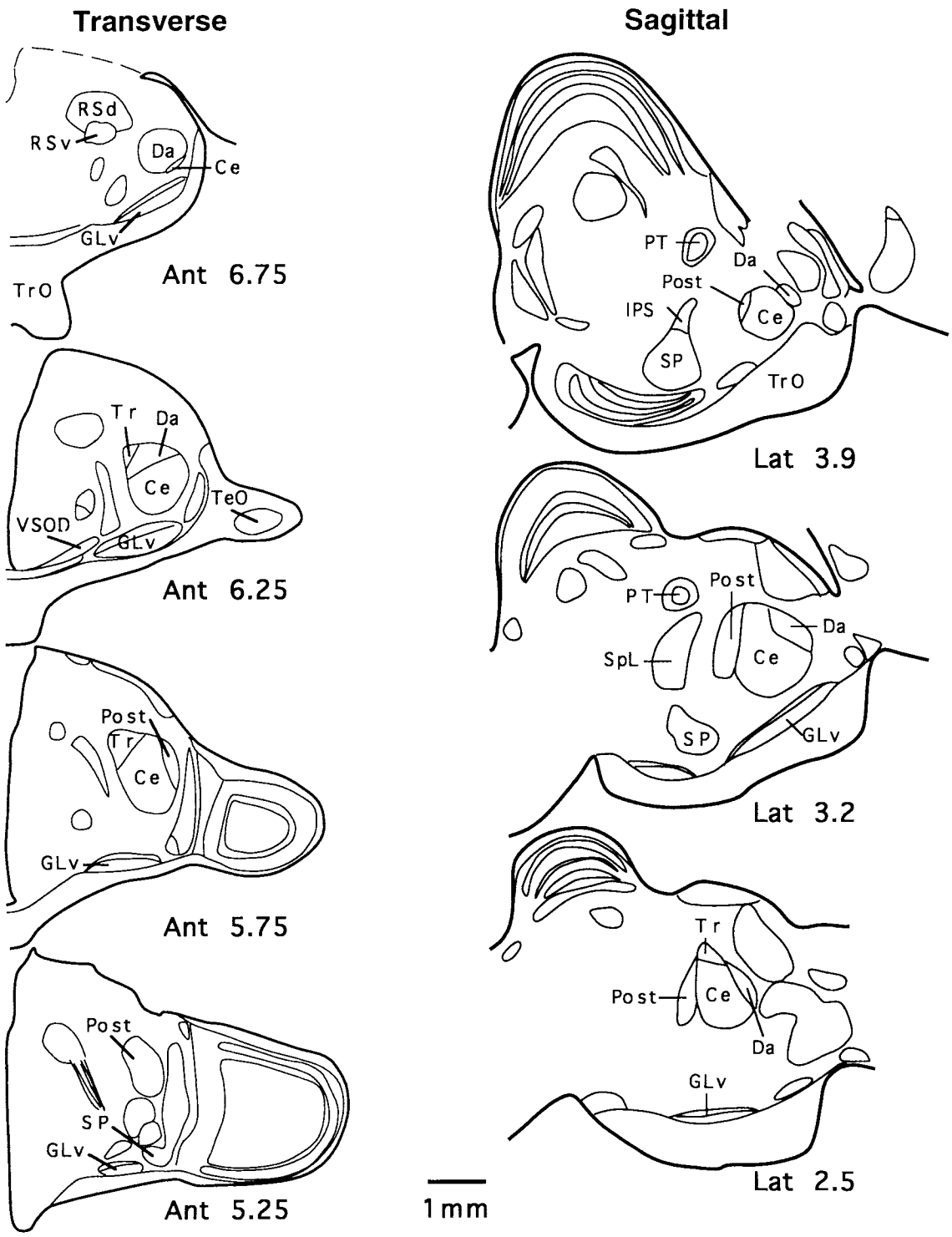

Fig. 1. Drawings of selected sections of the thalamus of the pigeon, showing the four major subdivisions (Da, Ce, Tr, and Post) of the rotundus. Drawings are based on acetylcholinesterase, parvalbumin, and calcium binding protein immunoreacted sections as well as in Nissl and Giemsa stained sections. Legend to the right of each drawing indicates the approximate stereotaxic level of the corresponding section (Karten and Hodos, 1967). Transverse sections are on the left, sagittal sections on the right. In this and all subsequent figures, abbreviations follow the conventions indicated in the Abbreviations section. Scale bar applies to all drawings in this figure.

ris or to the pars posterior divisions of the rotundus, there was intense labeling of the neurons of the ipsilateral SPcd, whereas an axonal plexus was labeled bilaterally (Figs. 6 and 9). SPcd was not labeled ipsilaterally or contralaterally following injections of retrograde tracer limited to the dorsoanterior or central divisions of the rotundus.

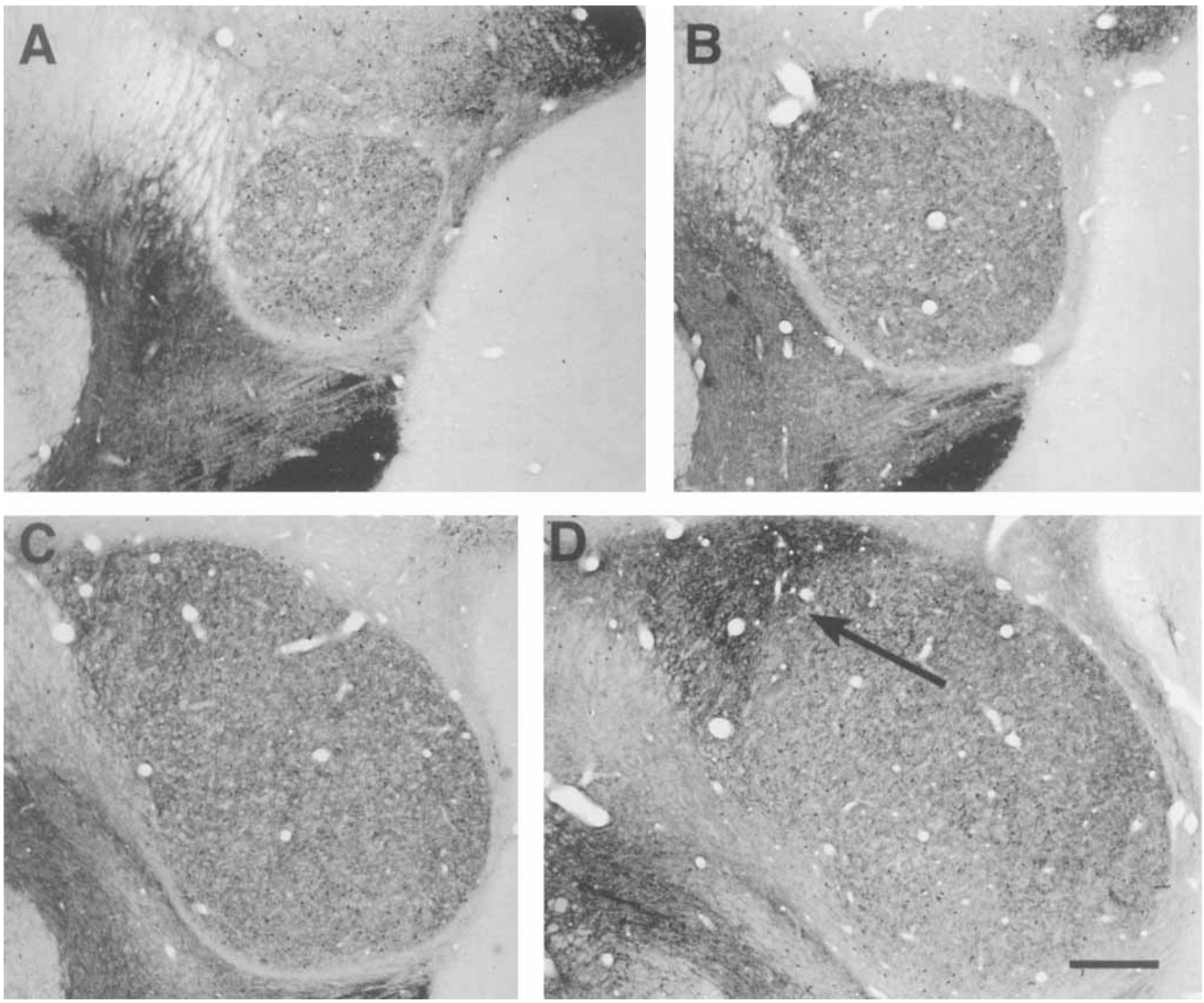

Fig. 2. Glutamic acid decarboxylase (GAD) immunoreactivity in the rotundus of the pigeon. Photomicrographs **A**, **B**, **C**, and **D** were taken at progressively more caudal levels through the nucleus, corresponding to the drawings shown in Figure 1. All the subdivisions of the rotundus appear intensely stained. Note the relatively higher intensity of staining in the pars triangularis (arrow in **D**). Scale bar = 440μm in D and applies to A-D.

Nucleus posteroventralis. Nucleus posteroventralis (PV) lies on the posteroventral to ventromedial margin of the rotundus. The cells of ipsilateral PV were intensely retrogradely cholera toxin B-labeled following unilateral injections within all the divisions of the rotundus. Dense axonal labeling was also observed within the ipsilateral and contralateral PV (Figs. 7 and 9).

Nucleus reticularis superior thalami, pars dorsalis, and pars ventralis (RSd and RSv). The cell group within the anterior diencephalon that has been designated as the nucleus reticularis superior thalami contains two subdivisions, pars dorsalis and pars ventralis. Both of these components lie within the fascicles of the ascending thalamotelencephalic component of the lateral forebrain bundle. Following unilateral injections within each subdivision of the rotundus, cells of these nuclei were found to be intensely retrogradely labeled on the ipsilateral side. There was no noticeable axonal label within RSd or RSv after these injections in either the ipsilateral or the contralateral sides (Figs. 8 and 9).

Control injection sites

Because the rotundus is located deep within the brain and is surrounded by the OPT, the optic tectum, and the overlying telencephalon, control injections were placed in each of these locations to determine the extent of the overlap of retrograde labeling within cell groups projecting upon the rotundus, which might potentially interfere with our interpretation of the histologic findings. In the following section, specific observations will be limited to results that were pertinent to the interpretation of the injections within the rotundus.

Optic tectum (15 Animals). The tectum is the source of the major input to the rotundus. However, there was no

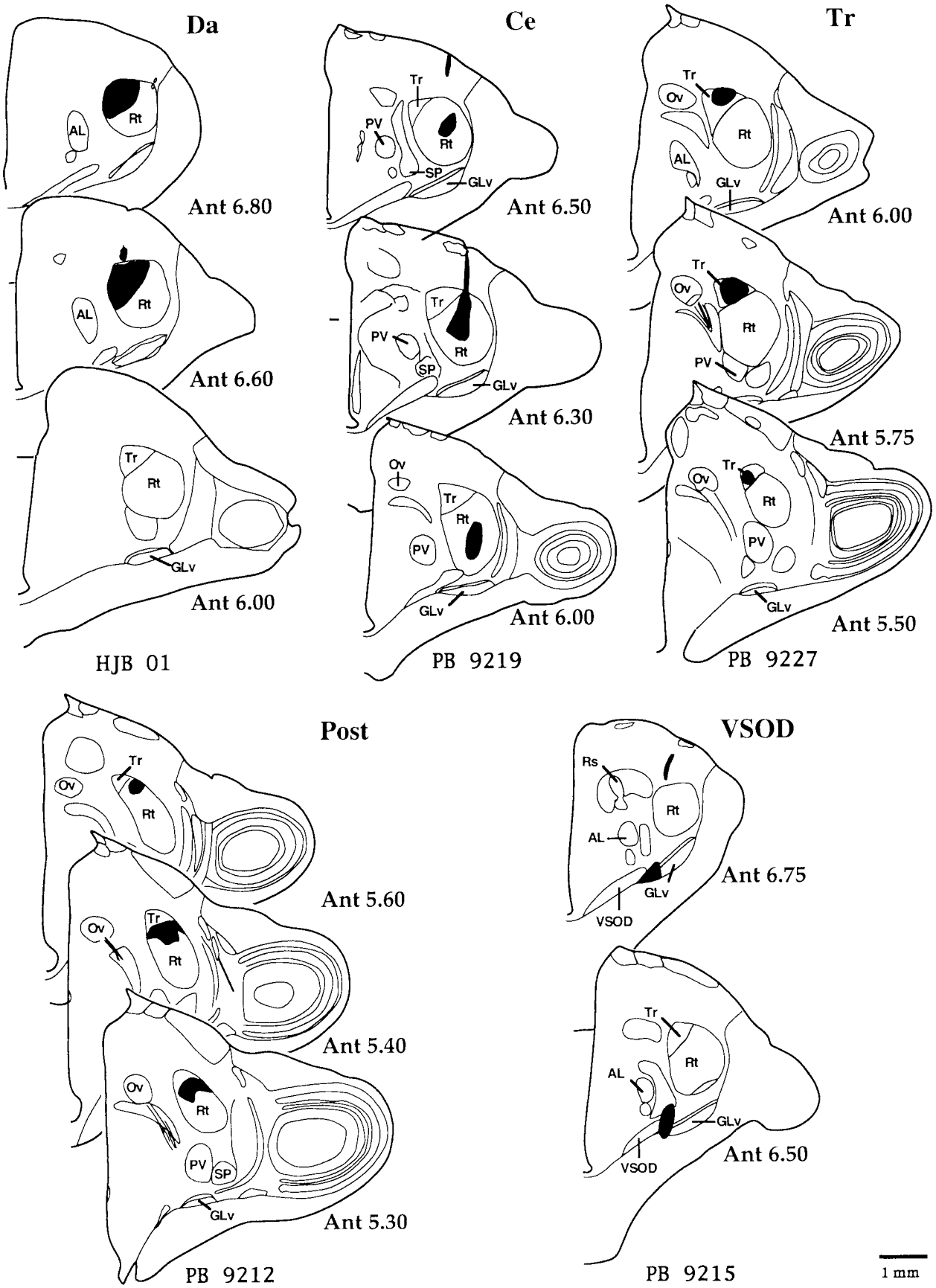

Fig. 3. Representative examples of cholera toxin B subunit injections in Da, Ce, Tr, and Post subdivisions of the rotundus and in the ventral supraoptic decussation (VSOD) are shown. In each case a series of drawings of selected transverse sections is shown. Solid black represents the actual injection sites. The legend at the bottom of each series identifies the case. Approximate anterior-posterior stereotaxic levels are indicated at the right of each drawing. Scale bar applies to all drawings in the figure.

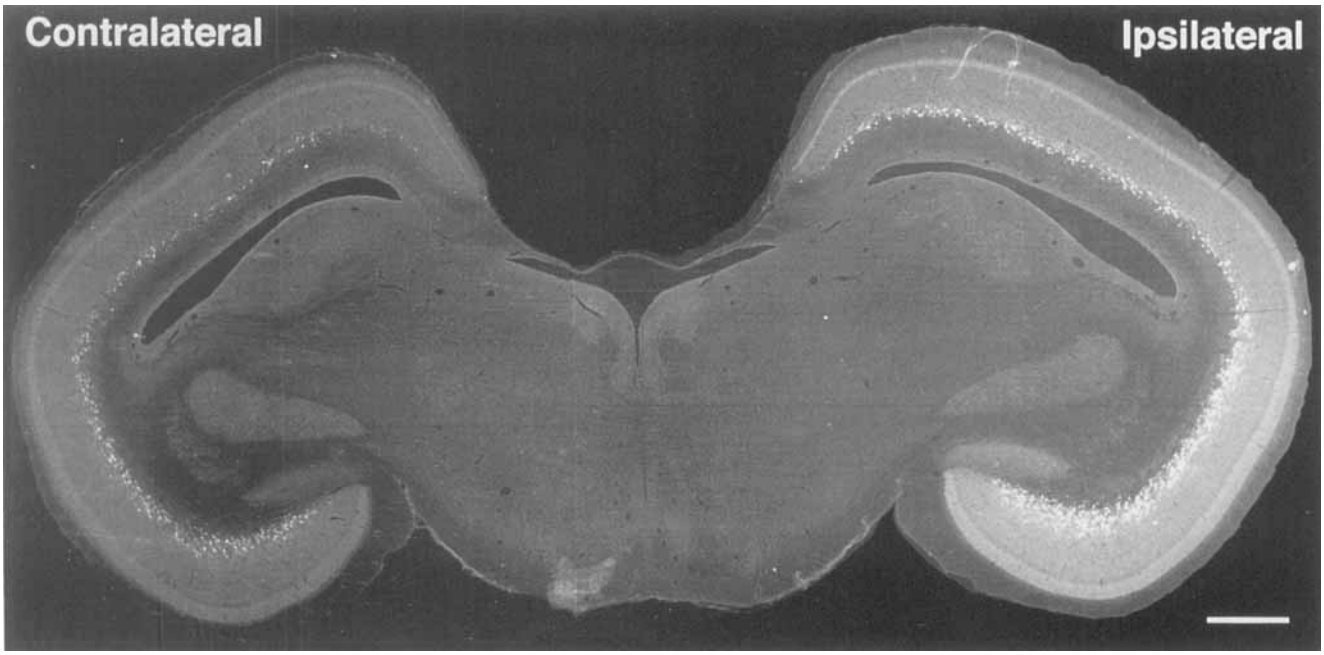

Fig. 4. Retrograde bilateral labeling of the optic tectum following a unilateral injection of cholera toxin B into the rotundus, showing the contralateral and ipsilateral sides. This is a low-power digital composition taken from a cholera toxin B immunoreacted section. In this case the injection was into the pars centralis of the rotundus (shown in Fig. 3, PB 9219). Note the bilateral distribution of retrogradely labeled neurons that were restricted to layer 13 and the greater density of cells on the side ipsilateral to the injection site. Contrast inverted to produce dark-field appearance. Scale bar = 900 μm.

retrograde cholera toxin B labeling of neurons within the rotundus, thus indicating the lack of a reciprocal projection of the rotundus upon the tectum. Similarly, the SP, IPS, PV, and reticularis superior thalami (RS) do not project upon the tectum, as indicated by the lack of retrograde labeling of these cell groups following cholera toxin B injections into various regions of the optic tectum.

Nucleus opticus principalis thalami (4 animals). Nucleus opticus principalis thalami (OPT) received a small input from the optic tectum. This input appeared to originate from the more superficial layers of the tectum and not from layer 13/SGC. There were no retrogradely labeled cells in the intrinsic nuclei of the tecto-thalamic tract.

Ventral nucleus of the lateral geniculate (GLv) (8 animals). Tectal neurons projecting upon GLv were seemingly restricted to layer 10 of the optic tectum. Injections confined to GLv did not retrogradely label cells of layer 13/SGC unless the cholera toxin B had spread into the overlying rotundus. Similarly, there were no retrogradely labeled neurons within the SP, IPS, or PV following injections of cholera toxin B into the GLv. This was further supported by the experiments, described below, of lesions of the SP/IPS and their effect on GAD-IR.

Telencephalon. We found no evidence of anterograde projections upon the rotundus proper in numerous experimental studies of the projections and the organization of the pigeon telencephalon. There was a sparse projection confined to the external capsule that surrounds the rotundus, seemingly arising from a subnucleus of the archistriatum. The optic tectum, the intrinsic nuclei of the tecto-thalamic tract, and the RS did not project directly upon the telencephalon.

Table I summarizes the distribution of retrogradely labeled neurons following injections into various subdivisions of the rotundus.

Source of GAD-IR within rotundus

Normal distribution of GAD-IR within cell groups projecting upon rotundus. As indicated previously, cells projecting upon the rotundus were found within three major neuronal groups: 1) layer 13/SGC of the ipsilateral and contralateral optic tectum, 2) intrinsic nuclei of the ipsilateral tecto-thalamic tract, and 3) nuclei reticularis superior, pars dorsalis and ventralis. The following section describes the distribution of GAD-IR found within each of these nuclei. There was no indication of any intrinsic cells within the rotundus that contained GAD-IR.

Layer 13/SGC. The distribution of GAD-IR in the optic tectum was complex. For purposes of the present report, we shall restrict our comments to layer 13/SGC. We found that all cells in layer 13/SGC were not immunoreactive for GAD. This was in distinct contrast to the pattern of immunoreactivity found in the small cells in the superficial layers (Fig. 10).

Intrinsic nuclei of tecto-thalamic tract. The neurons of SP, SPcd, IPS, and PV were all intensely GAD-IR. GAD-IR filled cells and many of their dendrites. The staining was most notable with antibody GAD 1440. Antibody GAD-2 produced punctate staining around the somata of these nuclei, but never the intense somatic staining characteristic of GAD 1440. These cell groups were among the most intensely GAD-IR neurons in the brain. (Fig. 10).

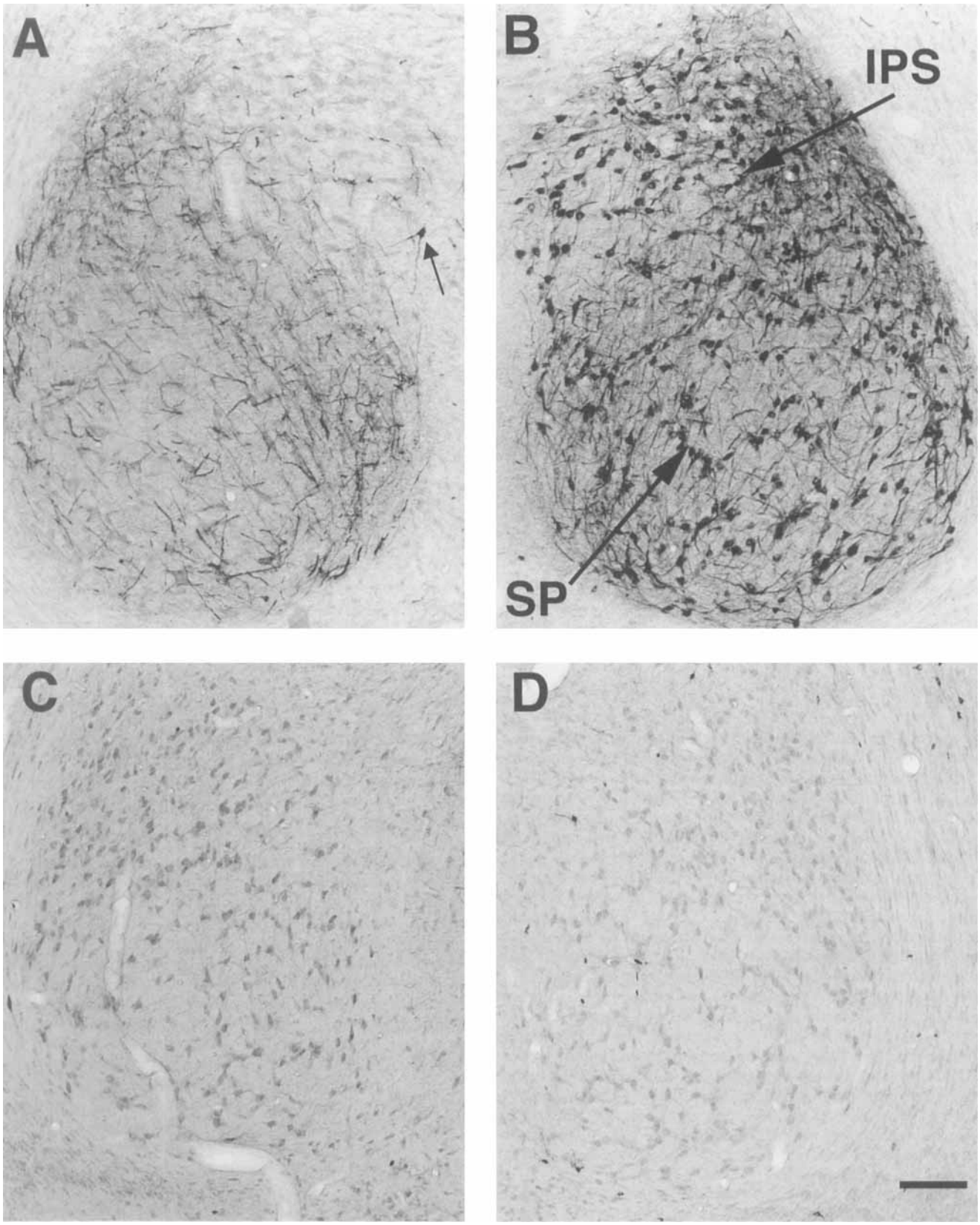

Fig. 5. Bilateral labeling of the subpretectalis/interstitio-pretecto-subpretectalis (SP/IPS) complex following injections of cholera toxin B into different subdivisions of the rotundus. Digital images were taken from cholera toxin B immunoreacted, Giemsa counterstained, transverse sections. This figure shows the pattern of cholera toxin B immunoreactivity in the contralateral (**A**) and ipsilateral (**B**) SP/IPS following a unilateral injection of cholera toxin B into pars centralis of the rotundus (shown in Fig. 3, PB 9219). Note that the labeled somata were restricted to the ipsilateral SP/IPS, whereas the axonal labeling was evident ipsilaterally and contralaterally. A single labeled neuron can be seen in A (arrow). Photomicrographs **C** and **D** show the lack of cholera toxin B-immunoreactivity in both the contralateral (C) and the ipsilateral (D) SP/IPS, following a unilateral injection of cholera toxin B into the pars posterior of rotundus (shown in Fig. 3, PB 9212). Despite the relatively dark Giemsa staining of some somata in C, there was no evidence of cholera toxin B labeling. See text and Figure 6 for comparison. Scale bar = 170 μm in D and applies to A-D.

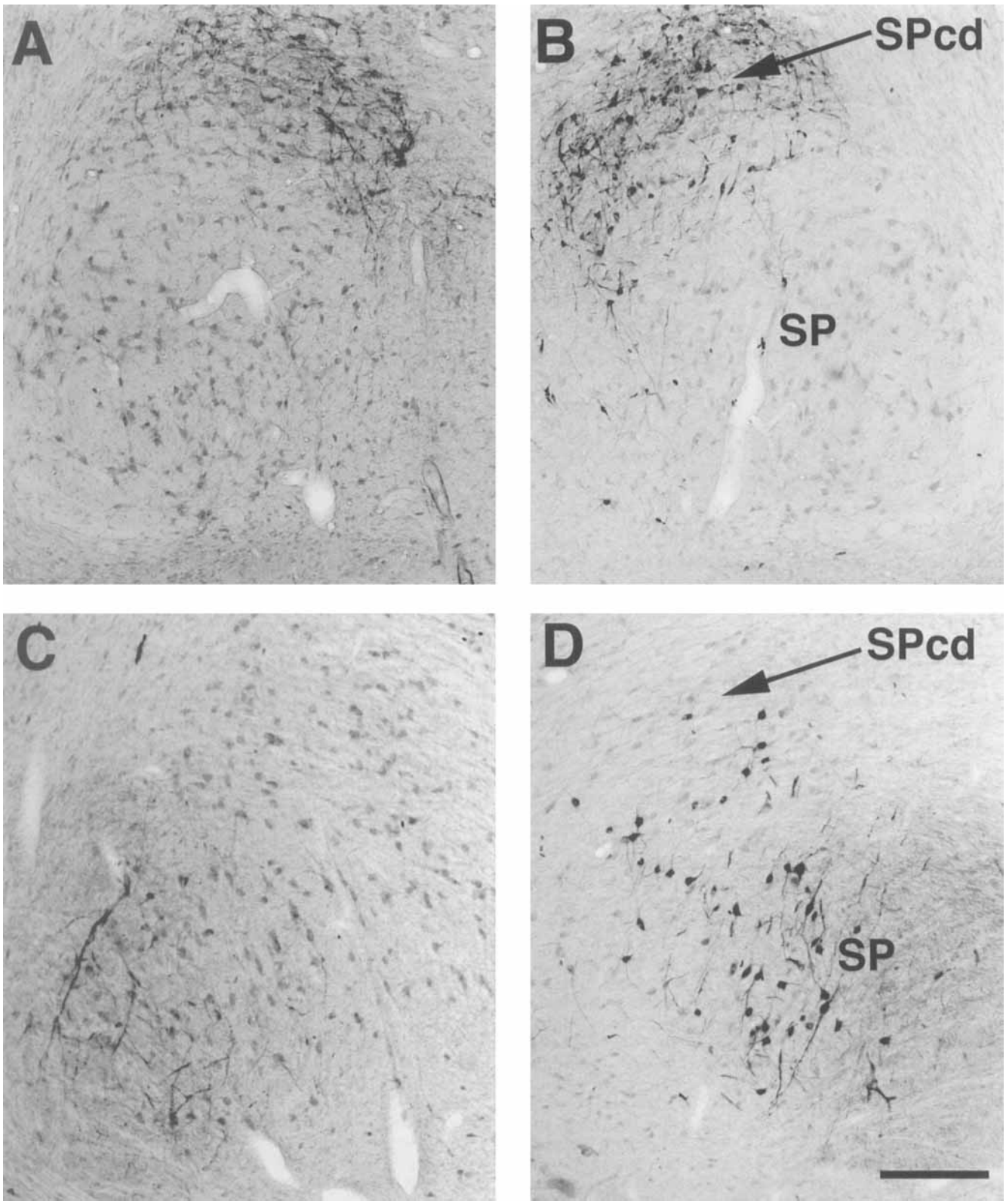

Fig. 6. Bilateral labeling of SPcd following injections of cholera toxin B into various subdivisions of the rotundus. Digital images were taken from cholera toxin B immunoreacted, Giemsa counterstained, transverse sections. **A** and **B** show the pattern of labeling of the contralateral (A) and the ipsilateral (B) nucleus subpretectalis, pars caudalis (SPcd) following a unilateral injection of cholera toxin B into the pars triangularis of the rotundus (shown in Fig. 3, PB 9227). Note that the retrogradely labeled somata were restricted to the ipsilateral SPcd, whereas the axonal staining was evident in both the ipsilateral and the contralateral SPcd. Photomicrographs **C** and **D** show the lack of cholera toxin B immunoreactivity in both the contralateral (C) and the ipsilateral (D) SPcd following a unilateral injection of cholera toxin B into pars anterior of the rotundus (shown in Fig. 3, HJB 01). Scale bar = 160 μm in D and applies to A-D.

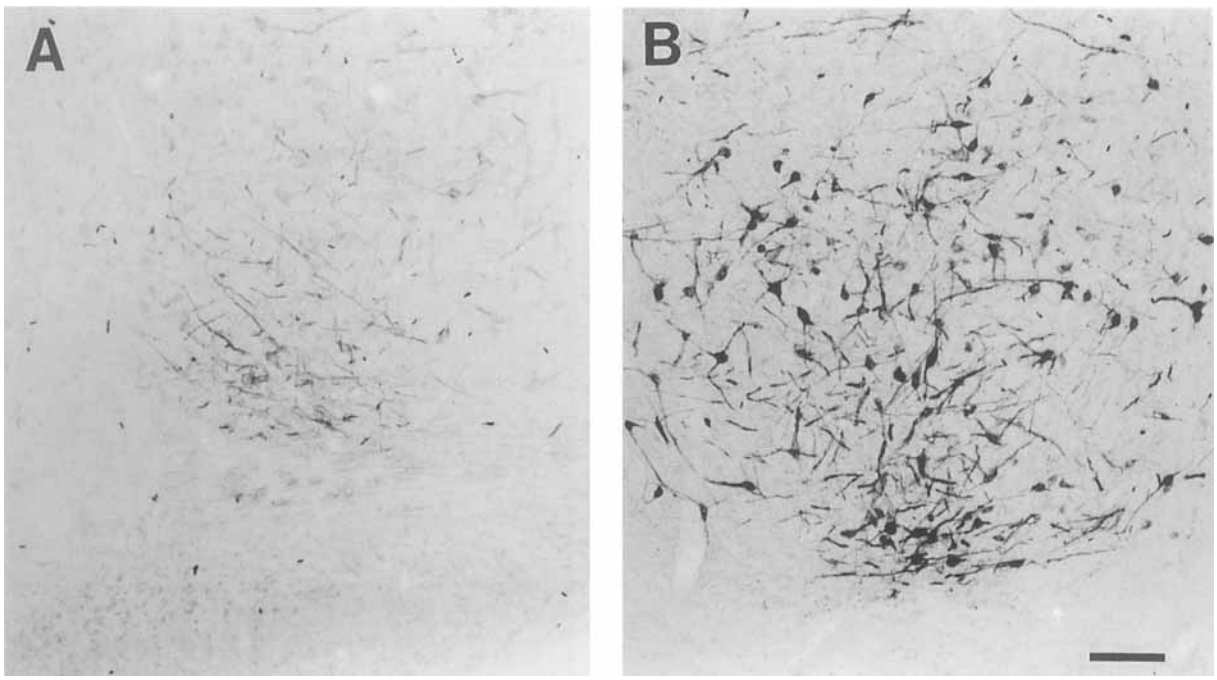

Fig. 7. Contralateral (**A**) and ipsilateral (**B**) nucleus posteroventralis thalami (PV) following unilateral injections of cholera toxin B into the rotundus. Photomicrographs were taken from cholera toxin B subunit immunoreacted transverse sections. The injection site in this case is shown in Figure 3, PB 9219. Note the intense labeling of axons, somata, and their dendrites in the ipsilateral PV. Only axons (sparse in this case) were cholera toxin B-labeled in the contralateral PV. Injections in other subdivisions of the rotundus produced a pattern of bilateral labeling in the PV that is similar to the one shown in this figure. Scale bar = 130 μm in B and also applies to A.

Nucleus reticularis superior, pars dorsalis and ventralis. RSd and RSv were intensely GAD-IR. The cells of RSd were large polygonal cells. Those of RSv were smaller and somewhat round. RS has also been found to project upon other thalamic cells groups, including nucleus ovoidalis (Fig. 9).

Table II summarizes the distribution of GAD-IR in these cell groups.

Destruction of SP/IPS: effect on GAD-IR within rotundus. Electrolytic lesions of the ipsilateral SP/IPS resulted in a major reduction in GAD-IR in the ipsilateral rotundus. Ipsilateral lesions appeared to have little effect on the intensity of GAD-IR within the contralateral rotundus when compared with the intensity of staining in the adjacent nuclei such as the GLv (Fig. 11). Absolute levels of GAD-IR were not measured. We were unable to obtain complete abolition of GAD-IR within the rotundus following SP/IPS lesions. We interpreted this to be due to the presence of the remaining GAD-IR cells in PV and RS.

Axonal labeling in the contralateral rotundus and afferents to the intrinsic nuclei of tecto-thalamic tract. Unilateral injections of cholera toxin B into the rotundus resulted in anterograde axonal labeling within the ipsilateral ectostriatum. In addition, a dense plexus of axonal processes was observed in the contralateral rotundus, topographically corresponding to the locus of the injection site. However, no retrogradely labeled neurons were observed in the contralateral rotundus (Fig. 12). This observation was further supported by injections of the anterograde tracer PHA-L into the rotundus. In these cases, the rotundal-ectostriatal efferent projection was clearly labeled, but no axonal labeling was observed in the contralateral rotundus, the ipsilateral or contralateral nuclei of tecto-thalamic tract, or the RS formation. These studies demonstrated that the efferent projections of the rotundus were restricted to the ipsilateral ectostriatal region of the telencephalon. They also indicated that the axonal labeling observed bilaterally in the nuclei of tecto-thalamic tract, and contralaterally in the rotundus, after unilateral injections of cholera toxin B into the rotundus was not of rotundal origin. Rather, such axonal labeling was the result of retrograde axonal transport along a group of neurons that project upon the rotundus, with subsequent anterograde labeling of their axonal collateral branches upon the nuclei of tecto-thalamic tract.

This axonal labeling originated from the optic tectum, as the tectum was the only structure that contains bilateral cellular labeling following cholera toxin B injections into the rotundus. We therefore examined the tectal efferent projections in our collection of tectal cholera toxin B injections. In agreement with previous observations (Karten and Revzin, 1966; Hunt and Künzle, 1976), we found that the intrinsic nuclei of tecto-thalamic tract received a major input from the ipsilateral optic tectum. The density of the input from the contralateral optic tectum differed within each nucleus of the group. Thus, PV received a moderately dense input from the contralateral tectum, whereas SP, SPcd, and IPS received only a very sparse contribution. We assumed from these observations that the tectal inputs to the intrinsic nuclei of tecto-thalamic tract were derived as axon collaterals of the cells of layer 13 that project bilaterally upon the rotundus. This interpretation accounts for the pattern of retrograde axonal labeling observed after the unilateral injections of cholera toxin B into the rotundus.

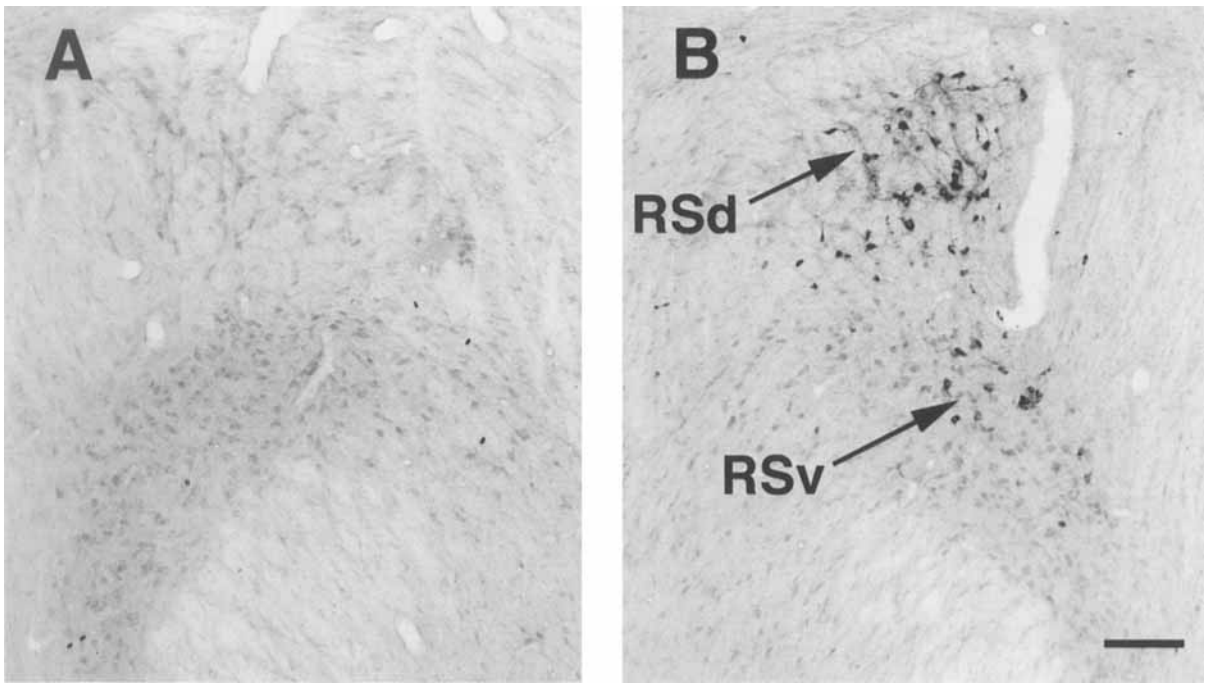

Fig. 8. Contralateral (**A**) and ipsilateral (**B**) nucleus reticularis superior (RS) complex following unilateral injections of cholera toxin B into the rotundus. Digital images were taken from cholera toxin B immunoreacted, Giemsa counterstained, transverse sections. The injection site in this case is shown in Figure 3, PB 9227. There is dense labeling of somata and processes in both the nucleus reticularis superior, pars dorsalis (RSd) and nucleus reticularis superior, pars ventralis (RSv). Giemsa counterstain readily demonstrates that only a portion of the small-celled RSv is retrogradely labeled, consequent to a limited injection site within the thalamus. Injections in the other subdivisions of the rotundus produced a pattern of bilateral labeling in the RS complex that is similar to the one shown in this figure. Scale bar equals 100 μm in B and also applies to A.

To confirm this interpretation, we placed a unilateral injection of cholera toxin B into the tecto-thalamic tract at the level of the visual supraoptic decussation (Fig. 13). Retrograde labeling of the tectum was restricted to the cells of layer 13 bilaterally. There were dense axonal arbors of equal density bilaterally in both the rotundus and the intrinsic nuclei of tecto-thalamic tract. There was no retrograde labeling of any of the neurons of these nuclei, supporting our previous statement that these gamma-aminobutyric acid (GABA)ergic neurons only projected on the ipsilateral thalamus. The axons in the contralateral nuclei of the tecto-thalamic tract are believed to be a mixture of anterogradely and retrogradely labeled processes. The anterograde axons are derived from the ipsilateral layer 13, and the retrogradely axons are those of the contralateral layer 13. These findings demonstrated that layer 13 is the source of the tectal input to both the rotundus complex and the intrinsic nuclei of the tecto-thalamic tract.

In summary, based on these studies we concluded that: 1) intrinsic nuclei of the tecto-thalamic tract received inputs from the layer 13/SGC neurons of the optic tectum, 2) these inputs were mainly ipsilateral, and 3) these inputs originated from collateral branches of the axons of the layer 13/SGC cells that projected bilaterally upon the rotundus. Our observations to date have not resolved the possibility that the intrinsic nuclei of the tecto-thalamic tract may receive an additional input from a population of layer 13/SGC neurons different from those that terminate within the rotundus proper.

DISCUSSION

The present report is mainly confined to a description of the GAD components of the tecto-rotundal system and to compare those components with direct inputs from the optic tectum.

Origin of GAD within rotundus

Distinctive axonal GAD-IR was found throughout all divisions of the rotundus, with a somewhat greater density found within the anterodorsal subdivision. Similar results were obtained using both a polyclonal sheep anti-human GAD antibody, GAD 1440, and a monoclonal mouse anti-chick GAD antibody, GAD-2. There was no indication of GAD-IR within rotundal neurons. Thus, we propose that all the GAD axonal immunoreactivity within the rotundus was of exogenous origin.

Exogenous sources of GAD axons within rotundus. In chicks, Csillag (1991) reports the presence of GAD-IR neurons within the ectostriatum—the telencephalic projection zone of the rotundus. However, there is no evidence of a reciprocal projection from the ectostriatum back upon the rotundus. Furthermore, despite numerous studies of the telencephalic projections, we have not found any evidence that the telencephalon projects upon the rotundus.

Similarly, although there were many GAD-IR neurons in the optic tectum, the tectum does not provide any direct GABA inputs to the rotundus. The tectal projections upon the rotundus originated exclusively from the neurons of

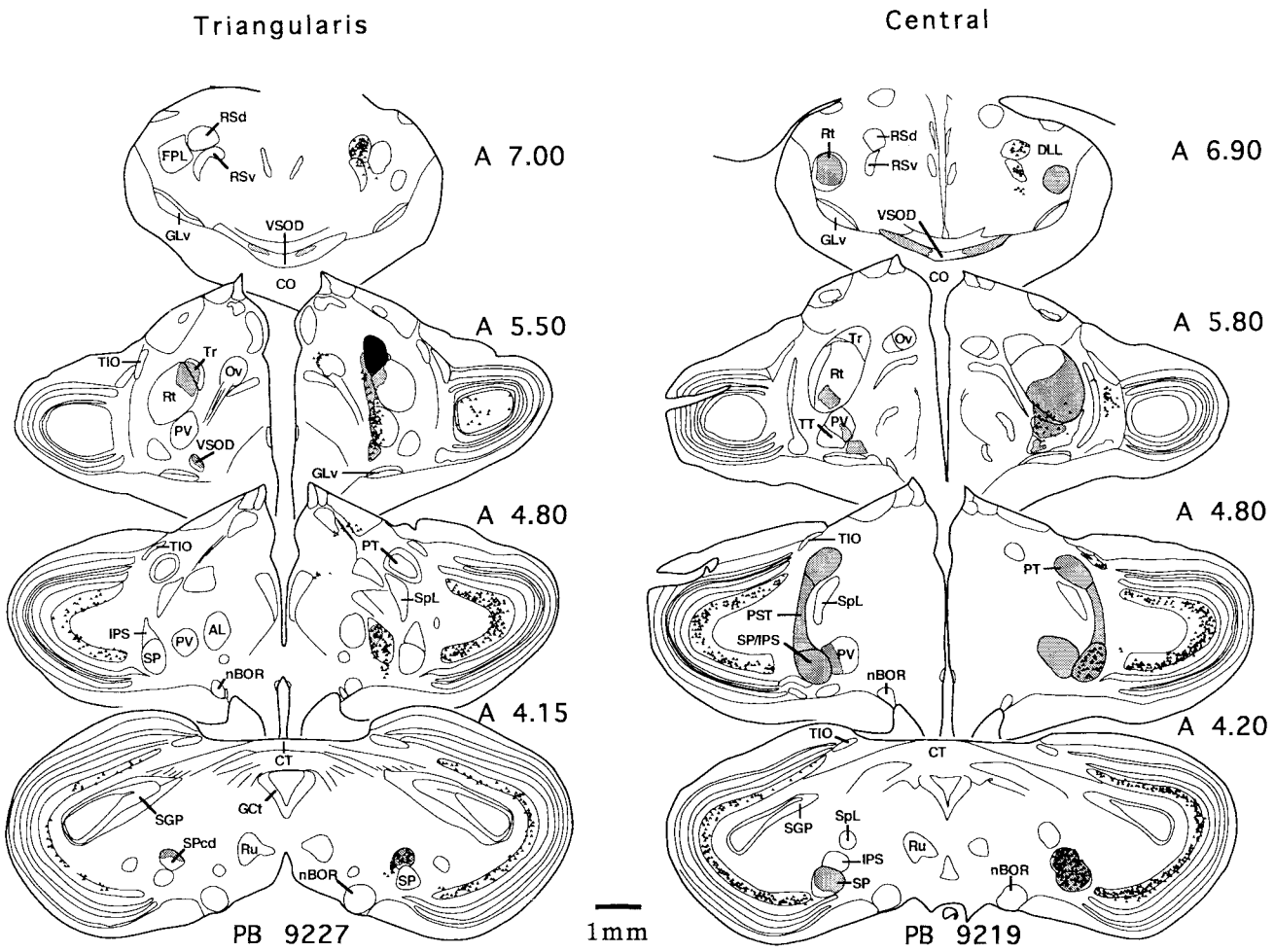

Fig. 9. Pattern of somata and axonal labeling following injections of cholera toxin B into different subdivisions of the rotundus. In each case a series of drawings of selected transverse sections are shown. Legends at the bottom of each series identify the cases. The injection site of each case is shown in Figure 3. Approximate anterior-posterior stereotaxic levels are indicated at the right of each drawing. Solid black triangles mark the location of labeled somata. Dotted areas indicate axonal labeling. Note that retrogradely labeled neurons in the RS, PV, SP/IPS, and SPcd are restricted to the ipsilateral side. Axonal transport is found bilaterally in the rotundus, PV, SP/IPS, and SPcd. In the triangularis injection, cellular and axonal labeling is not found in the SP/IPS but is found in the SPcd. In the central injection, the result is the opposite. Note the bundle of labeled axons that progress in the dorsal direction from the SP/IPS to the nucleus pretectalis (PT) in the central injection case. Scale bar applies to all drawings in this figure.

TABLE 1. Distribution Of Retrogradely Labeled Neurons Following Injections Into Rotundus Subdivisions

	SGC	SP	SPcd	IPS	PV	RS d/v
RtDa	+	+	−	+	+	+
RtCe	+	+	−	+	+	+
RtPost	+	−	+	−	+	+
RtTr	+	−	+	−	+	+

layer 13/SGC. The cells of layer 13/SGC did not show any immunoreactivity for GAD.

Using ultrastructural techniques in chicks, Ngo et al. (1992) identifies a group of terminals on the soma and the main proximal dendrites of rotundal neurons that formed symmetric synapses and contained flattened vesicles. These synapses were shown to be immunoreactive for GABA. Ngo et al. suggest that the sources of GABAergic fibers seem to be the subpretectal and the ventral posterior thalamic nuclei. This suggestion is further supported by the studies of chicks by Tombol et al. (1994), showing that the incoming fibers to the rotundus from the SP and PV nuclei were GABAergic. The present study confirms and extends these findings regarding the source of the GABA inputs to the rotundus. Our results revealed that the GAD-IR within the rotundus was derived from the axons of the SP, SPcd, IPS, PV, and RS and recognized specific inputs from some of these nuclei to the different subdivisions of the rotundus. This was based on the differential retrograde labeling of these cell groups from the subdivisions of the rotundus and on the presence of intense immunoreactivity for GAD in the somata of each of these nuclei. This was further supported by the marked reduction of GAD-IR found within the rotundus following the destruction of the ipsilateral SP/IPS/SPcd complex. Residual GAD-IR observed within the rotundal axons was attributable to the remaining contribution from the PV and RSd/RSv. Furthermore, we attempted to label axons of the SP/IPS directly using PHA-L and then to double label the sections for GAD-IR using fluorescent

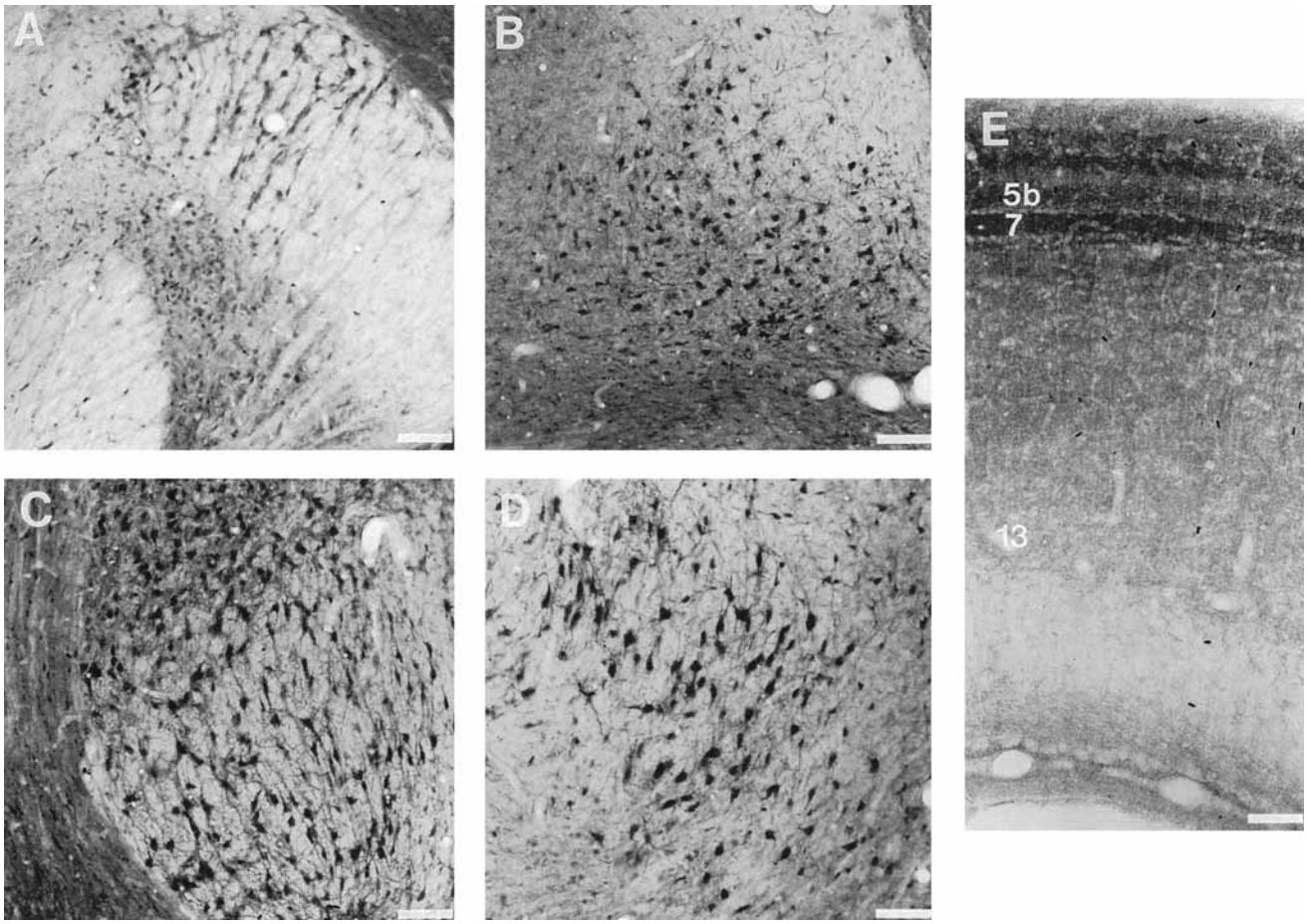

Fig. 10. GAD immunoreactivity in afferents into the rotundus. Photomicrographs were taken from a series of GAD immunoreacted transverse sections. All somata of the RSd and RSv (**A**), PV (**B**), SP/IPS (**C**), and SPcd (**D**) are labeled. GAD immunoreactivity in the optic tectum (**E**) is mainly seen in the superficial neuropil, with greatest density in the retino-recipient layers 2–7. There was no evident immunoreactivity for GAD in the large neurons of layer 13. Layer 14, the layer of tectal efferent axons projecting upon the rotundus, is generally lacking in significant levels of axonal GAD immunoreactivity. Scale bar = 135 μm in A and B, 107 μm in C and D, and 175 μm in E. In E, tectal layers are indicated.

TABLE 2. GAD-IR In Somata Of Nuclei Projecting Upon Rotundus

	SGC	SP	SPcd	IPS	PV	RS d/v
GAD-IR	–	+	+	+	+	+

secondary antibodies. Numerous individual axons stained for both PHA-L and GAD were found. However, the overall density of staining for both substances was substantial; hence, it was difficult to obtain satisfactory photographs showing the presence of both labels within single axons.

We have made preliminary observations using various antibodies directed against mammalian GABA receptors. Our results to date have revealed that cells in all subdivisions of the rotundus express GABA-A receptors.

Afferent connections of subdivisions of rotundus

This study extends the previous results of Benowitz and Karten (1976) with respect to the major sources of input to the rotundus complex. They correctly suggest that the tectal inputs to different subdivisions of the rotundus derive from different sublaminae of layer 13/SGC. A forthcoming paper will deal with this issue in greater detail. They also indicate that the SP/IPS and RS project upon the rotundus. However, there are several significant differences between Benowitz and Karten (1976) and the present study. They suggest that the SP/IPS projects upon a distinct subnucleus of the rotundus, and that the "ventral" and "anteroventrolateral" region in receipt of the SP/IPS projection does not receive any input from the tectum. They also report that the triangular and the posterior divisions of the rotundus do not receive input from the SP/IPS. Although they were correct in this latter conclusion, they failed to recognize the input to the triangular and the posterior divisions from the SPcd. Our present analysis indicated that all regions of the rotundus received a direct input from the tectum. All divisions of the rotundus also received input from the SP/IPS or SPcd complex. Benowitz and Karten (1976) did not comment on the presence of cells within the PV projecting upon the rotundus. The present study did not address the matter of projections of the

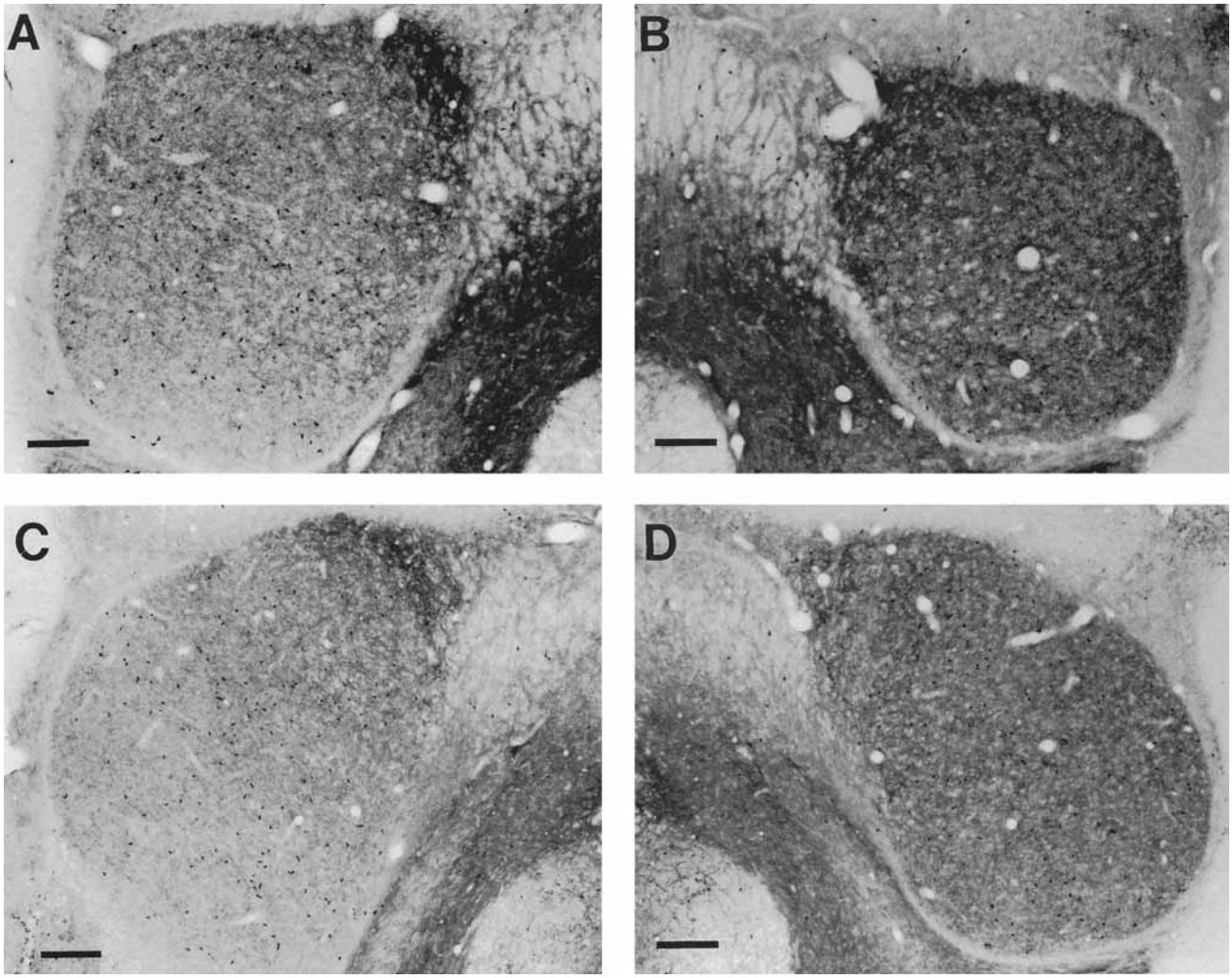

Fig. 11. Consequences of a unilateral lesion of the SP/IPS complex on GAD immunoreactivity within the rotundus. Following a unilateral electrolytic ablation of the SP/IPS (not shown), photomicrographs of GAD immunoreacted transverse sections through the rotundus were taken bilaterally at anterior (**A** and **B**) and mediocaudal (**C** and **D**) levels. The lesioned hemisphere is shown at left (A and C), and the normal hemisphere at right (B and D). Note the marked loss of GAD immunoreactivity in the rotundus at the lesioned side. The intensity of staining in adjacent areas of the diencephalon is not altered by this lesion. Scale bar equals 180 μm in A, 220 μm in B-D.

rotundus upon the telencephalon. We hope to address that issue in a forthcoming study.

Intrinsic nuclei of the tecto-thalamic tract (SP, SPcd, IPS, PV)

The SP, SPcd, IPS, and PV all lie within the main bundle of tectal efferent fibers and together are called the intrinsic nuclei of the tecto-thalamic tract. These intrinsic nuclei all received inputs from the tectum, but did not receive any direct retinal inputs to their somata or proximal dendrites. The present study demonstrated that the tectal inputs have now been shown to arise as collaterals of axons of tectal neurons in layer 13/SGC in transit to the rotundus. The present results also demonstrated that the SP and IPS both projected upon anterior and central divisions of the rotundus, and the SPcd projected upon the triangular and posterior portions of the rotundus. The specific pattern of axonal arborization within the rotundus of each contributing nucleus must still be addressed in future studies.

Nucleus reticularis superior

In addition to the projections of RS upon rotundus, RSd and RSv also projected upon the nucleus ovoidalis and possibly other cell groups within the thalamus. By comparison, our findings indicated that the intrinsic nuclei of the tecto-thalamic tract projected only upon the rotundus. The RSd and RSv did not appear to project upon the telencephalon, nor did they receive any direct inputs from the optic tectum. This supports the possibility that the RS of the avian thalamus is similar to the nucleus reticularis thalami of mammals.

Organization and interactions of transmitters in the ascending tecto-thalamic pathway

The present findings suggested a complex pattern of organization of transmitters in the ascending tectal pathways to the rotundus, with major differences in the influ-

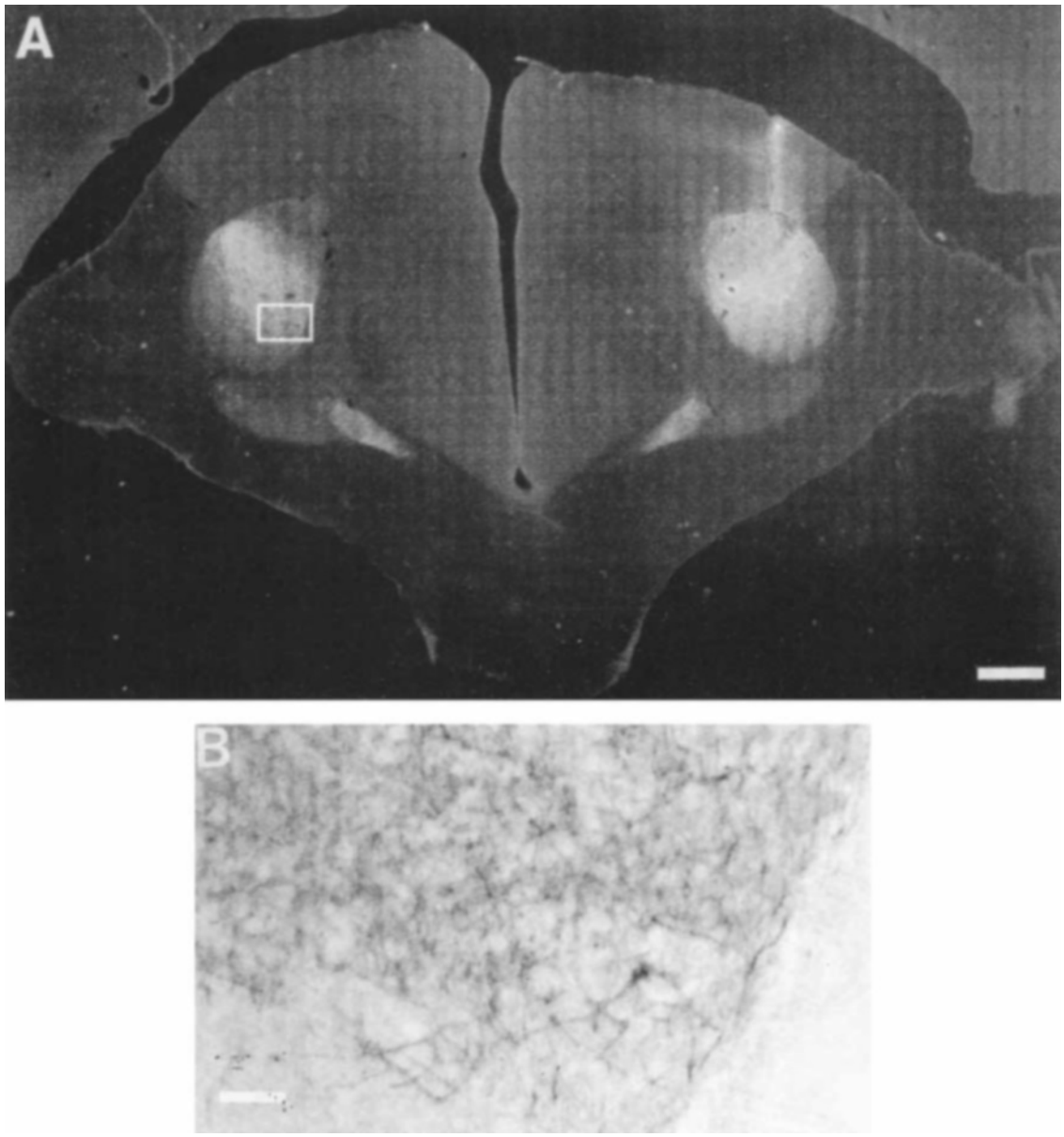

Fig. 12. (**A**) A low-power digital image of a cholera toxin B immunoreacted section showing the site of an injection of cholera toxin B into the pars centralis of the rotundus. The main locus of the injection (right side) corresponds to the area of greatest brightness. The adjacent labeled zones within the right rotundus represent axonal transport of the tracer. Note that on the contralateral side, there is axonal cholera toxin B labeling of rotundus restricted to the region corresponding to the loci of the injection site. Clear bilateral labeling of the VSOD can be noted as well. (**B**) A detailed digital image of the region indicated in rectangle on A, showing axonal arborization within the contralateral rotundus. Individual neurons are outlined by axonal arbors, but no retrograde somatic cholera toxin B labeling was observed. Scale bars = 660 μm in A, 110 μm in B.

ence of the tectum on the ipsilateral and contralateral rotundus.

The input to the rotundus from layer 13 of the tectum was not immunoreactive for GAD, choline acetyltransferase, catecholamines, and all the common neuropeptides for which we have antibodies (including substance P, enkephalin, neuropeptide Y, neurotensin, vasoactive intestinal polypeptide, somatostatin, and bombesin) (Karten and Mpodozis, unpublished observations).

Ngo et al. (1994) propose that tectal neurons provide an excitatory input to the rotundus based on the presence within the rotundus of presynaptic terminals with spherical vesicles presumed to have a tectal origin. Dye and Karten (1993) conclude that the direct tectal projections of layer 13 upon the rotundus are excitatory and mediated by glutamate. Using slice preparations of the chick brain, they report that stimulation of the optic tectum results in excitatory field potentials within the rotundus of the chick. Since the cells of layer 13 project bilaterally upon the rotundus, we suggest that the influence of the direct tectal terminations within the rotundus are excitatory in both the ipsilateral and contralateral rotundus.

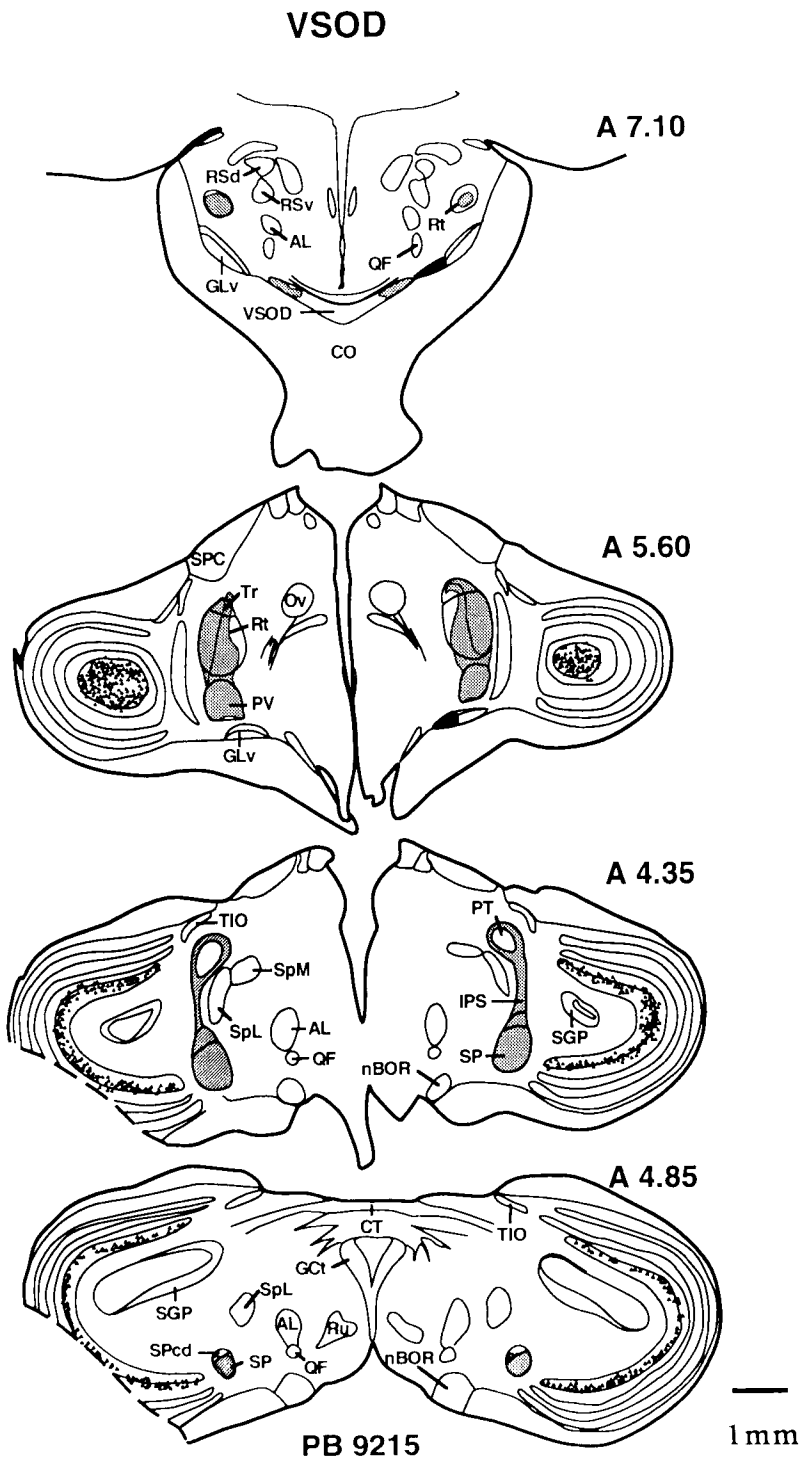

Figure 13. Pattern of somata and axonal labeling following injections of cholera toxin B into VSOD. A series of drawings of selected transverse sections of case PB 9215 are shown. Injection site is shown in Figure 3. Approximate anterior-posterior stereotaxic levels are indicated at the right of each drawing. Solid black circles mark the location of labeled somata, and dotted areas indicate axonal labeling. Note that the pattern of axonal distribution in the rotundus, PV, SP/IPS, and SPcd is similar to that observed following injections into the rotundus (Fig. 9). However, retrogradely labeled somata are restricted to layer 13 of the optic tectum. In this instance, unlike those cases with limited ipsilateral injections in rotundus, the relative density of labeled somata in the tectum is approximately equal on both sides. Scale bar applies to all drawings in the figure.

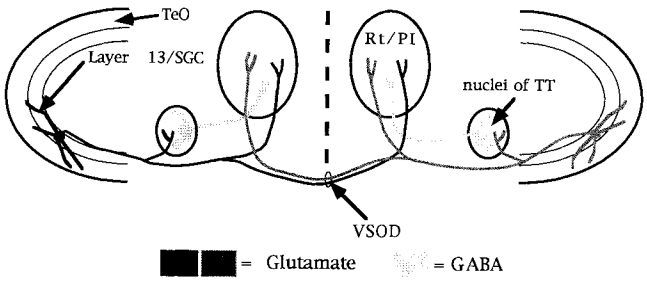

Figure 14. Schematic summary of tectal glutaminergic and pretectal GABAergic inputs into the rotundus complex. The rotundus receives a dense bilateral tectal/glutaminergic input from neurons of layer 13 of the optic tectum. These tectal axons also terminate, mainly ipsilaterally, as collateral branches on the GABAergic neurons of the SP/IPS, SPcd, and PV. The GABAergic neurons of the SP/IPS, SPcd, and PV terminate in the ipsilateral rotundus. See text for further discussion.

The projections of layer 13/SGC neurons end upon the ipsilateral GAD-IR intrinsic nuclei of the tecto-thalamic tract. The present study provided direct evidence that the terminations of layer 13 neurons upon the intrinsic nuclei are collaterals of axons projecting to the rotundus. The postsynaptic projections of the GAD-IR intrinsic nuclei provided a massive GABAergic input to the ipsilateral rotundus, presumably of inhibitory nature. However, this effect was mainly restricted to the ipsilateral rotundus. A small projection of the tecto-thalamic tract upon the contralateral PV was observed, with only sparse terminations observed upon the contralateral SP/SPcd/IPS.

Thus, tectal neurons provided excitatory inputs bilaterally upon the rotundal neurons. The ipsilateral layer 13 neurons also activated a GABAergic input into the rotundus, but only on the ipsilateral side and following a synaptic delay. These inputs are summarized in Figure 14.

The present study supports the proposal of Benowitz and Karten (1976) that the inputs from the SP/IPS are likely to be inhibitory. However, in contrast to their interpretation that the SP/IPS projects upon rotundal regions that differ from those receiving tectal input, we would now suggest that the SP/IPS/SPcd projects upon all regions of the rotundus complex and overlaps with the primary tectal terminations within the rotundus.

Physiological and behavioral implications

Bilateral interactions in the tecto-rotundal system. One of the most prominent of features of the tecto-rotundal pathway is the presence of a bilateral projection upon the thalamus from the midbrain. Although this pathway initially was considered to be unique, Diamond (1973) repeatedly showed the existence of an identical pathway in several different species of mammals, including tree shrews, squirrels, and hedgehogs. Abplanalp (1970), Revzin and Karten (1967), Benowitz and Karten (1976), Hunt and Künzle (1976), Engelage and Bischof (1988, 1993), and Ngo et al. (1994) all provide evidence of the presence of a bilateral tecto-rotundal pathway in pigeons and chicks.

Despite the prominence of the bilateral tectal projections upon the rotundus, most physiologic studies of the rotundus, with the exception of the studies by Bischof and colleagues (Engelage and Bischof, 1988; Bishof and Niemann, 1990; Herrmann and Bischof, 1986; Engelage and Bischof, 1993), have failed to recognize any binocular interactions in the visual responses of the neurons of the tecto-rotundal-ectostriatal pathway.

Engelage and Bischof (1988) observe that stimulation of the ipsilateral retina produces a minimal response in the ectostriatum, but no response could be detected within the rotundus unless the contralateral retina was removed. Bilateral visual stimulation produces excitatory responses in both the rotundus and the ectostriatum that are indistinguishable from those obtained following contralateral stimulation alone. They suggest that the *ipsilateral retinal* influence on the rotundus is inhibited by the activity of the contralateral retinal pathway.

Our study found a notable difference between the primary tectal projections upon the rotundus and the projections from the intrinsic nuclei of the tecto-thalamic tract. The tectal projections were bilateral, whereas the projections from the SP/IPS complex were exclusively ipsilateral. This indicated that the tectum can excite rotundal neurons bilaterally, but only activated the inhibitory GABAergic system of the ipsilateral side. As the GABA is presumably inhibitory, we propose the results that Engelage and Bischof (1988) reflect the actions of the intrinsic nuclei of the tecto-thalamic tract upon the rotundal neurons. The microcircuitry of such actions might require that the axons of GABAergic neurons from nuclei of the tecto-thalamic tract terminate selectively upon the input from the contralateral optic tectum. However, in the absence of more precise information about the domains of arborization of single tectal and intrinsic tecto-thalamic tract neurons, we cannot suggest a specific role for this circuit in generating the complex response properties of the rotundal neurons described by Revzin (1979) or Wang et al. (1993).

Does SP/IPS act as a delay for temporal sharpening of responses?

One of the most striking physiologic observations of the response properties of the rotundal neurons in birds has been the exquisite sensitivity of rotundal neurons to extremely small displacements of visual stimuli. This property is probably due to a complex series of processing steps in the retina, the tectum and the rotundus.

The connections of layer 13/SGC neurons provide both a direct excitatory and an indirect inhibitory projection upon the neurons of the rotundus, as described above. This arrangement may provide a sequential excitatory input, followed by a temporally precise delay before the arrival of the GABAergic inhibitory input. Such an arrangement would serve to sharpen the transient nature of the retino-tectal-rotundal input. This would dampen the initial response to a stimulus and prime the rotundal neurons for a renewed response to a fresh incoming stimulus.

Comparison with mammals

The rotundus appears to be homologous with the inferior/caudal pulvinar of squirrels and tree shrews (Raczkowski and Diamond, 1978, 1981). A more detailed discussion of this relationship is presented in Shimizu and Karten (1993) and in a forthcoming paper on the tecto-rotundal system. The caudal pulvinar of squirrels receives a bilateral input from the SGC cells of the superior colliculus. The caudal pulvinar contains GAD-IR axons; however, the source of these axons is unknown. Although we may presume that a portion of these axons arise from the nucleus reticularis thalami, as in the present study, other possible contribu-

tions from GABAergic pretectal cell groups must also be considered.

Without precise information about the topography of the tecto-nuclei of the tecto-thalamic tract-rotundus pathway, and the possible juxtaposition of directly projecting axons upon individual rotundal neurons, we can only speculate about the influence of the direct excitatory inputs and the indirect inhibitory inputs. We may, however, presume that this interaction, simultaneously modified by an excitatory input from the contralateral tectum, must play a significant role in determining the response properties of the rotundal neurons.

ACKNOWLEDGMENTS

The authors gratefully acknowledge the excellent technical assistance of Agnieszka Brzozowska-Prechtl. This work was supported by grants Fondecyt 1081 to J.M., and NEI EY-06890 and NINDS NS 24560 to H.J.K.

LITERATURE CITED

Abplanalp, P. (1970) Some subcortical connections of the visual system in tree shrews and squirrels. Brain Behav. Evol. *3*:155–168.

Benowitz, L.I., and H.J. Karten (1976) Organization of the tectofugal visual pathway in the pigeon: A retrograde transport study. J. Comp. Neurol. *167*:503–520.

Bischof, H.-J., and J. Niemann (1990) Contralateral projections of the optic tectum in the zebra finch (*Taeniopygia gutta castanotis*) Cell Tissue Res. *262*:307–313.

Britto, L.R., D.E. Hamassaki-Britto, E.S. Ferro, K.T. Keyser, H.J. Karten, and J.M. Lindstrom (1992) Neurons of the chick brain and retina expressing both alpha-bungarotoxin-sensitive and alpha-bungarotoxin-insensitive nicotinic acetylcholine receptors: An immunohistochemical analysis. Brain Res. *590*:193–200.

Csillag, A. (1991) Large GABA cells of chick ectostriatum: Anatomical evidence suggesting a double GABAergic disinhibitory mechanism. An electron microscopic immunocytochemical study. J. Neurocytol. *20*:518–528.

Diamond, I.T. (1973) The evolution of the tectal-pulvinar system in mammals: Structural and behavioral studies of the visual system. Symp. Zool. Soc. London *33*:205–333.

Dye, J.C., and H.J. Karten (1993) An in vitro slice preparation of tectofugal visual pathways in the chick. Soc. Neurosci. Abstr. *19*:767.

Engelage, J., and H.J. Bischof (1988) Enucleation enhances ipsilateral flash evoked responses in the ectostriatum of the zebra finch (*Taeniopygia guttata castanotis* Gould). Exp. Brain Res. *70*:79–89.

Engelage, J., and H.J. Bischof (1993) The organization of the tectofugal pathway in birds: A comparative review. In Ziegler H.P., and H.J. Bischof (eds): Vision Brain and Behavior in Birds. Cambridge: MIT Press, pp. 137–158.

Gerfen, C.R., and P.E. Sawchenko (1983) An anterograde neuroanatomical tracing method that shows the detailed morphology of neurons, their axons and terminals: Immunohistochemical localization of an axonally transported plant lectin *Phaseolus vulgaris* leucoagglutinin. Brain Res. *290*:219–238.

Gottlieb, D.I., Y.-C. Chang, and J.E. Schwob (1986) Monoclonal antibodies to glutamic acid decarboxylase. Proc. Natl. Acad. Sci. USA *83*:8808–8812.

Granda, A.M., and S. Yazulla (1971) The spectral sensitivity of single units in the nucleus rotundus of pigeon, *Columba livia*. J. Gen. Physiol. *57*:363–384.

Herrmann, K., and H.J. Bischof (1986) Effects of monocular deprivation in the nucleus rotundus of zebra finches: A nissl and deoxyglucose study. Exp. Brain Res. *64*:119–126.

Hodos, W., and H.J. Karten (1966) Brightness and pattern discrimination deficits in the pigeon after lesions of nucleus rotundus. Exp Brain Res *2*:151–167.

Hodos, W., and H.J. Karten (1970) Visual intensity and pattern discrimination deficits after lesions of ectostriatum in pigeons. J. Comp. Neurol. *140*:53–68.

Hunt, S.P., and H. Künzle (1976) Observations on the projections and intrinsic organization of the pigeon optic tectum: An autoradiographic study based on anterograde and retrograde, axonal and dendritic flow. J. Comp. Neurol. *170*:153–172.

Iñiguez, C., M.J. Gayoso, and J. Carreres (1985) A versatile and simple method for staining nervous tissue using Giemsa dye. J. Neurosci. Methods *13*:77–86.

Karten, H.J., and W. Hodos (1967) A Stereotaxic Atlas of the Brain of the Pigeon (*Columba livia*). Baltimore: Johns Hopkins Press.

Karten, H.J., and W. Hodos (1970) Telencephalic projections of the nucleus rotundus in the pigeon (*Columba livia*). J. Comp. Neurol. *140*:35–52.

Karten, H.J., and A.M. Revzin (1966) The afferent connections of the nucleus rotundus in the pigeon. Brain Res. *2*:368–377.

Karten, H.J., K. Cox, J. Mpodozis, H.J. Bischof, and T. Shimizu (1993) Little cells ending on big cells: An oligosynaptic retino-tecto-pulvinar system in pigeon. Soc. Neurosci. Abstr. *19*:969.

Kuhlenbeck, H. (1939) The development and structure of the pretectal cell masses in the chick. J. Comp. Neurol. *71*:361–388.

Ngo, T.D., A. Nemeth, and T. Tombol (1992) Some data on GABAergic innervation of nucleus rotundus in chicks. J. Hirnforsch. *33*:335–355.

Ngo, T.D., D.C. Davies, G.Y. Egedi, and T. Tombol (1994) A Phaseolus lectin anterograde tracing study of the tecto-rotundal projections in the domestic chick. J. Anat. *184*:129–136.

Oertel, W.H., D.E. Schmechel, M.J. Brownstein, M.L. Tappaz, D.H. Ransom, and I.J. Kopin (1981) Decrease of glutamate decarboxylase (GAD)-immunoreactive nerve terminals in the substantia nigra after kainic acid lesion of the striatum. J. Histochem. Cytochem. *8*:977–980.

Raczkowski, D., and I.T. Diamond (1978) Cells of origin of several efferent pathways from the superior colliculus in Galago senegalensis. Brain Res. *146*:351–357.

Raczkowski, D., and I.T. Diamond (1981) Projections from the superior colliculus and the neocortex to the pulvinar nucleus in Galago. J. Comp. Neurol. *200*:231–254.

Reiner, A., and A.S. Powers (1980) The effects of extensive forebrain lesions on visual discriminative performance in turtles (*Chrysemys picta picta*). Brain Res. *192*:327–337.

Reiner, A., H.J. Karten, and N.C. Brecha (1982) Enkephalin-mediated basal ganglia influences over the optic tectum: Immunohistochemistry of the tectum and the lateral spiriform nucleus in pigeon. J. Comp. Neurol. *208*:37–53.

Revzin, A.M. (1979) Functional localization in the nucleus rotundus. In Granda A.M., and J.H. Maxwell (eds): Neural Mechanisms of Behavior in the Pigeon. New York: Plenum Press, pp. 175.

Revzin, A.M., and H.J. Karten (1967) Rostral projections of the optic tectum and the nucleus rotundus in the pigeon. Brain Res. *3*:264–276.

Shimizu, T., and H.J. Karten (1991) Central visual pathways in reptiles and birds: Evolution of the visual system. In Cronly-Dillon J.R., and R.L. Gregory (eds): Evolution of the Eye and Visual System, Volume 2. Boca Raton: CRC Press, pp. 421–441.

Shimizu, T., and H.J. Karten (1993) The avian visual system and the evolution of the neocortex. In Zeigler H.P., and H.-J. Bischof (eds): Vision, Brain, and Behavior in Birds. Cambridge: MIT Press, pp. 103–114.

Shimizu, T., H.J. Karten, and W. Woodson (1988) GABAergic inputs to the nucleus rotundus in pigeons (*Columba livia*). Soc. Neurosci. Abstr *14*:991.

Swanson, L.W., J. Lindstrom, S. Tzartos, L.C. Schmued, D.D. O'Leary, and W.M. Cowan (1983) Immunohistochemical localization of monoclonal antibodies to the nicotinic acetylcholine receptor in chick midbrain. Proc. Natl. Acad. Sci. USA *80*:4532–4536.

Tombol, T., G. Egedi, and A. Nemeth (1994) Phaseolus vulgaris lectin labeled and GABA immunogold stained terminals in nucleus rotundus: An EM study. J. Hirnforsch. *35*:233–252.

Wang, Y.C., S. Jiang, and B.J. Frost (1993) Visual processing in pigeon nucleus rotundus: Luminance, color, motion, and looming subdivisions. Vis. Neurosci. *10*:21–30.